

1 Endophytic fungus *Alternaria macrospora*: A promising and eco-friendly source for
2 controlling *Aedes aegypti* and its toxicity assessment on non-targeted organism, zebrafish
3 (*Danio rerio*) embryos

4 Chinnasamy Ragavendran^{1*}, Chinnaperumal Kamaraj², Devarajan Natarajan³, Ismini
5 Nakouti⁴, Tijo Cherian⁵, Venkatesan Manigandan⁶, Kumar Manimaran⁷, Guilherme
6 Malafaia⁸

7
8 ¹Department of Cariology, Saveetha Dental College and Hospitals, Saveetha Institute of
9 Medical and Technical Sciences (SIMATS), Saveetha University, Chennai-600 077,
10 Tamil Nadu, India

11 ²Interdisciplinary Institute of Indian System of Medicine (IIISM), Directorate of Research
12 and Virtual Education, SRM Institute of Science and Technology (SRMIST),
13 Kattankulathur, Chennai-603203, Tamil Nadu, India

14 ³Natural Drug Research Laboratory, Department of Biotechnology, School of
15 Biosciences, Periyar University, Salem - 636 011, Tamil Nadu, India.

16 ⁴Centre for Natural Products Discovery (CNPD), School of Pharmacy and Biomolecular
17 Sciences, Liverpool John Moores University, Liverpool L3 3AF, UK.

18 ⁵School of Biosciences, Mar Athanasios College for Advanced Studies Tiruvalla
19 (MACFAST), Tiruvalla, Kerala-689101, India

20 ⁶University of Texas Health Science Center, San Antonio, TX, USA

21 ⁷Research Center for Applied Microbiology, National Research and Innovation Agency
22 (BRIN), Jl. Raya Bogor Km. 46, Cibinong 16911, Indonesia.

23 ⁸Laboratory of Toxicology Applied to the Environment, Goiano Federal Institute, Urutaí,
24 GO, Brazil. Post-Graduation Program in Conservation of Cerrado Natural Resources,
25 Goiano Federal Institute, Urutaí, GO, Brazil. Post-Graduation Program in Ecology,
26 Conservation, and Biodiversity, Federal University of Uberlândia, Uberlândia, MG,
27 Brazil. Post-Graduation Program in Biotechnology and Biodiversity, Federal University of
28 Goiás, Goiânia, GO, Brazil.

29
30 **Corresponding Author:**

31 ***Dr. Chinnasamy Ragavendran**, ¹Department of Cariology, Saveetha Dental College and
32 Hospitals, Saveetha Institute of Medical and Technical Sciences (SIMATS), Saveetha
33 University, Chennai-600 077, India, E-mail: ragavan889@gmail.com.

35

36 **ABSTRACT**

37 Fungal compounds are believed to be the most efficient method of addressing challenges
38 with pesticide resistance and contamination of the environment. The present study was
39 aimed to evaluate the larvicidal, pupicidal, ovicidal, histopathology profile, antibacterial,
40 cytotoxic effects of cervical cancerous cells and its toxicity assessments using zebrafish
41 embryo (*Danio rerio*). The isolates were confirmed by macroscopic, microscopic and
42 PCR using a universal internal transcribed spacer primer for the molecular identification
43 of the isolated fungus at the species level (GenBank - MN049541). The isolated fungus
44 was first tested for its ability to produce toxic compounds in *Aedes aegypti* larvae in the 1-
45 4th instar. For each instar of determined mosquito larvae, the secondary metabolites were
46 evaluated in different bioassays at different test concentrations (100 to 500 µg/mL). The
47 lethal concentrations of *A. macrospora* mycelial ethyl acetate extract that kill 50% of
48 exposed larvae (LC₅₀) and 90% of exposed larvae (LC₉₀) were found in the first, second,
49 third, and fourth instar larvae of *A. aegypti* (LC₅₀ = 96.167, 131.370, 217.595, and 143.864
50 µg/mL and (LC₉₀ = 395.16, 483.692, 882.545, and 655.722 µg/mL). After 120 h of
51 exposure, the ovicidal bioassay's mean (%) was observed. A dose-dependent pattern was
52 found in the enzymatic level of acetylcholinesterase in 4th instar larvae exposed to fungal
53 mycelial metabolites. The treatment of 500 µg/mL of mycelia metabolites produced
54 significant histopathological damage in the 4th instar mosquito larvae. The highest growth
55 inhibition zones were observed during the antibacterial investigation of *Alternaria*
56 *macrospora* metabolites against *E. coli* (22 mm) and *S. aureus* (20 mm). Also, the
57 detected mycelium metabolites were tested for docking studies to identify their binding
58 ability towards the *E. coli* FimH and *S. aureus* tyrosyl-RNA synthetase protein. The
59 mycelium metabolites with different concentrations were further tested in the *in-vivo*
60 zebrafish model to evaluate developmental toxicity. This is the first report on mosquito
61 larvicidal and pupicidal activity of ethyl acetate metabolites produced by *A.*
62 *macrospora* species. The study findings demonstrate that *A. macrospora* metabolites
63 might be an ideal, cheap, small, and environmentally suitable source for controlling *A.*
64 *aegypti* larvae.

65 **Keywords:** *Alternaria macrospora*, *Aedes aegypti*, Biopesticides, Endophytic fungus,
66 Zebrafish embryo,

67 1. INTRODUCTION

68 *Aedes aegypti* is the principal vector of human infections such as Dengue, Chikungunya fever,
69 and Zika virus (Lambrechts, 2023); this species is strongly related to human habitation, and some
70 epidemic patterns of the diseases transmitted by the species are driven by seasonal variations that
71 impact its growth, reproduction, and abundance (Pliego-Pliego et al., 2020). Due to population
72 growth, arboviruses transmitted by *A. aegypti* have become much more widespread during the past 50
73 years (Ferreira et al., 2023). Dengue causes over 100 million symptomatic illnesses yearly and 10,000
74 deaths in over 125 countries (Messina et al., 2019). Reducing the vector population is the major
75 approach to control because dengue or other illnesses caused by this vector may be managed (Pliego-
76 Pliego et al., 2020). Generally, organophosphate, carbamate, and pyrethroid insecticides are suggested
77 for use as traditional larvicides due to their low persistence in the environment (Khursheed et al.,
78 2022). The most widely used larvicides are the organophosphorus substances, effective against
79 mosquito larvae and other aquatic insects. Examples include temephos, fenthion, and chlorpyrifos
80 (Okagu et al., 2023). Temephos is the preferred larvicide for controlling *A. aegypti* and *Anopheles*
81 sp., whereas fenthion and chlorpyrifos are used to control *Culex* sp. species (Nithya et al., 2022). The
82 use of synthetic chemical pesticides, insect growth regulators, and chemical repellents for vector
83 control is increasing, and this leads to environmental contamination, adverse effects on non-targeted
84 organisms, and the development of insecticide resistance in mosquito species (Vivekanandhan et al.,
85 2022). This makes environmentally friendly, green pesticides necessary for the control of mosquitoes
86 (Chatterjee et al., 2023). Researchers have found beneficial compounds from biological sources, such
87 as microorganisms and plants, which contain substantial quantities of metabolites and essential oils.
88 The development and research of natural larvicidal products exclusively addresses the utilization of
89 larvicidal oils (Gupta & Gupta, 2022), plant extracts (Kumar et al., 2023; Álvarez Valverde et al.,
90 2022; Ganesan et al., 2023); microbial larvicides act as *Bacillus* spp., secondary metabolites, or more
91 expensive insect growth regulators as alternatives to synthetic pesticides.

92

93 Natural remedies produced from fungus or other biological sources are cost-effective, safe for
94 the environment, and effective in addressing these issues (Narayanankutty et al., 2021). Natural
95 products offer viable substitutes and potential supplies for several biological activities (Singab et al.,
96 2022). Microbes are a prosperous provider of bioactive secondary metabolites and are an opportunity
97 source of mosquito control agents like positive bacterial strains (*Bacillus thuringensis* var. *israelensis*
98 (*Bti*) and *B. sphaericus* (*Bs*) (da Silva Sa et al., 2023). These bacterial toxins are well-known for their
99 effective against mosquito larvae at a minimal dose and are inert and harmless to non-targeted
100 organisms (Patil et al., 2011). Finding effective and environmentally acceptable bio-larvicides is

101 essential for managing mosquitoes (John et al., 2022). Fungi-derived secondary metabolites can also
102 be an alternative to artificially formulated pesticides, as they are comparatively cheap and
103 biodegradable (Lorenzen & Anke, 1998). Numerous research has examined the potential application
104 of entomopathogenic fungi genera *Metarhizium*, *Beauveria*, *Coelomomyces*, and *Culicinomyces* in
105 the management of vector-borne illnesses (Kamareddine, 2012; Beltrán & Lozano, 2022).

106 Endophytes (endo-internal, phytes-flora) are microorganisms dwelling inside other organisms
107 without inflicting any soreness (Elawady et al., 2023). Endophytic fungi asymptotically live in the
108 inner tissues of flowers, under the epidermis, colonizing the healthy dwelling tissues through quiescent
109 infections (Lanfranco and Fiorilli et al., 2022; Sharma et al., 2022). The endophytic fungal species are
110 hosted in approximately 300,000 terrestrial flowers, each one web hosting one or greater endophytic
111 forms (Mohamed et al., 2023). The endophytic strains were distinct from one-of-a-kind varieties of
112 flora: timber (yew, pine), fodders (clover, alfalfa, sorghum), vegetables, culmination, cereals, and other
113 crops (Lu et al., 2012). They play a critical function in enhancing plant health, particularly as bio-
114 control agents in suppressing plant pest groups like bugs and pathogens (Xiang et al., 2016).
115 Endophytic fungi are known to possess antimicrobials and anticancer compounds like taxol furnishing
116 factors of significance in agriculture, pharmaceutical, medicine, and nanotechnology (Tapwal et al.,
117 2015; Santra & Banerjee, 2022; Joshi et al., 2017). These endophytes are well known for the
118 production of biologically active secondary metabolites namely, terpenoids, alkaloids, steroids,
119 isocoumarins, quinones, phenylpropanoids, lactones, lignans, and phenols (Santos et al., 2015).
120 Endophytic fungal strains of *Pseudotaeniolina globosa* and *Penicillium purpurogenum* are said as
121 larvicides (Seetharaman et al., 2017). *Trichoderma harzianum* is known to control tomato gray mold
122 resulting from *Botrytis cinerea*, without fungicide resistance and is environmentally benign (Pan et al.,
123 2016). The filamentous fungi possess a few advantages: clean to handle; require easy vitamins, have
124 excessive wall-binding capability, and have intracellular metal uptake competence (Araújo et al.,
125 2022).

126 Alarmingly, more individuals throughout worldwide suffer from health issues carried on by
127 different cancers, microbes that are resistant to drugs, parasitic protozoans, and fungus (Abdelaziz et
128 al., 2023). Drug-resistant diseases are becoming an urgent global issue (Jouda et al., 2016). The
129 emergence of several drug-resistant bacteria increased the demand for the discovery of novel and
130 potent antimicrobial drugs for the management of human diseases (Bacha et al., 2016). Endophytes
131 are a unique source of potentially beneficial medicinal products in the urgent search for stronger and
132 more powerful drugs to help with various diseases challenges (Xing et al., 2011; Toghueo, 2020).
133 Endophytic fungi have the potential to be a source of secondary metabolites that may be used to
134 develop new drugs, which makes them interesting from a biotechnological perspective (Sharma et al.

135 2016). Several investigations have demonstrated that plant endophytic fungi have antifungal and
136 antibacterial properties (Li et al., 2014; Kalimuthu et al., 2022; Santra et al., 2022). *Escherichia coli*
137 fimbria contain the bacterial adhesin protein FimH, which is responsible for attaching bacteria to their
138 host cells. FimH is therefore important in the development of drugs because it plays a key role in
139 bacterial infections such urinary tract infections (Magala et al., 2020). The production of charged
140 tRNAs by aminoacyl-tRNA synthetases is an essential phase in the production of proteins. An amino
141 acid is transported onto a corresponding tRNA to produce the desired product after being condensed
142 with an ATP molecule to generate a stable aminoacyl-adenylate intermediate. Because the synthetases
143 play such a crucial function, substances that selectively block bacterial aminoacyl-tRNA synthetases
144 might become effective antibacterial drugs (Sahiba et al., 2022). For example, multidrug-resistant *S.*
145 *aureus* can cause life-threatening infections that need to be addressed in a hospital.

146 One of the major causes of mortality in the entire world, cancer is on growing, with an
147 alarming increase in the number of people who become diagnosed with different cancers each year.
148 Due to various limitations, existing cancer drugs and treatments are associated with a high death rate
149 (Elghaffar et al., 2022). Cervical cancer is caused mostly by persistent infection with particular strains
150 of human papillomavirus (HPV) and affects women all over the world. The prevention, detection,
151 and treatment of cervical cancer present difficulties in many nations, including India (Chauhan et al.,
152 2020). In this context, endophytic compounds were evaluated for cytotoxic and antibacterial activities
153 in an attempt to find a safer and innovative medicine utilizing natural products (Katoch et al., 2017).
154 Almost 72% of the extracts exhibited cytotoxic action against one of the investigated cell lines, whereas
155 39% of the extracts were potent versus all of the tested cell lines with >50% inhibition of growth
156 (Hazalin et al., 2009; Vu et al., 2023). Because of their increased bio compatibility, easy absorption,
157 and improved delivery of medicines at specified target sites.

158 *Alternaria macrospora* (Zimm.) is the most important phyto-pathogen responsible for
159 *Alternaria* leaf spot disease in genetic cotton, with regional, national, and worldwide effects
160 (Manpreet Kaur et al., 2015). *Alternaria* spp. are often regarded as pests of agriculture. It is either
161 saprophytes or have developed to become effective phyto-pathogens that cause illnesses in a range of
162 host plants (Thomma, 2003; Guo et al., 2004). More than 70 various kinds of chemicals/toxins are
163 produced by different *Alternaria* sp. (EFSA, 2011; Sharma & Sharma, 2014). *Alternaria* sp. act as
164 various biological properties such as insecticidal activity (Podova et al., 1977; Kaur et al., 2013),
165 biocontrol agents (Ashutosh & Pati, 2011), antibacterial, antioxidant, antiviral and anticancer (Brase et
166 al., 2009; Tsuge et al., 2013; Elghaffar et al., 2022). The *Trichillia* genus (belonging to the family
167 Meliaceae), comprising about 419 plant species, possesses pharmacological and biological
168 propensities (de la Torre-Anzures et al., 2023). *Trichillia connaroides* (Wight and Arn, 1962), a

169 previous nomenclature named *Heynea trijuga* Roxb, has been used as a traditional remedy in South-
170 East Asia, India, and China (Cazal et al., 2023). It is a small evergreen tree widely distributed in South
171 and East Asia including India, Indonesia, and South China. In recent years, enormous research has
172 been related to the insecticidal and pharmacological efficacy of *Trichillia* sp., which possess biological
173 activities like insect antifeedant, insecticidal, and insect growth regulators, along with anti-microbial,
174 anti-malarial, anti-cancers, antiviral and different pharmacologic uses (de Souza Passos et al., 2022;
175 Kowa et al., 2022).

176 Additionally, potential compounds for the screening of novel insecticides for controlling *A.*
177 *aegypti* larvae should exhibit significant efficacy and low hazard to non-target aquatic species. The
178 zebrafish embryotoxicity test has been employed in drug screenings because it makes it feasible to
179 rapidly assess the toxicity of a broad spectrum of compounds. The screening procedure for
180 embryotoxicity used in the assessment of the toxicity of new substances is in accordance with the
181 standard for the OECD 236 guideline and is conducted in multiple well plates (OECD, 2013). The
182 zebrafish is an excellent animal model that is increasingly used for detecting the toxicity and safety of
183 chemicals and for *in-vivo* chemical potency screening (He et al., 2014). Currently, zebrafish screens
184 are used to examine a variety of environmental toxins, pharmaceutical agents, and compound
185 databases over a range of life phases, transgenic and mutant lines, test dosages, and exposure times
186 (Freitas et al., 2023). On the other hand, the zebrafish model shows promise as a practical alternative
187 to the mammalian models presently employed in toxicity testing and assessment (Nishimura et al.,
188 2015). Zebrafish are distinctive for their tiny size, optically clear embryos, quick embryonic
189 development, low care cost, high fertility, and closeness to mammalian systems (Selderslaghs et al.,
190 2013). Besides that, zebrafish larvae can be widely used for genetic and drug tests based on the entire
191 organism (Mamboungou et al., 2022). Thus, we aim to isolate, molecularly characterize, and evaluate
192 the mycelial metabolites of the endophytic fungus *Alternaria macrospora* from *Trichillia connaroides*
193 to determine them against *A. aegypti* larvicidal, ovicidal activity and its estimation of
194 acetylcholinesterase (AChE) activity. Additionally, to assess the ecotoxicological potential of the fungi
195 metabolites produced by *A. macrospora* for aquatic species, we investigated their toxicity in zebrafish
196 embryos (*Danio rerio*). The antimicrobial potential of the fungi metabolites is identified by their
197 amino interaction with the *Escherichia coli* FimH protein and *Staphylococcus aureus* tyrosyl-RNA
198 synthetase protein. On a vertebrate model, we suggest that an endophytic *A. macrospora* fungal
199 extract might be used to control selected mosquito larvae with hard effects.

200

201 **2. MATERIAL AND METHODS**

202 **2.1. Collection of plant material**

203 Fresh leaves of *T. connaroides* were collected from the Botanical Survey of India (BSI) in
204 Yercaud (Latitude: 11.7893931; Longitude: 78.216629), Salem (District), Tamil Nadu, India. Dr. D.
205 Natarajan, Assistant Professor, Periyar University, Tamil Nadu, India, performed the taxonomy
206 identification. The receipt for the specimen of the obtained sample was deposited with the Natural
207 Drug Research Laboratory (NDRL), Periyar University, Salem, India (specimen number:
208 PU/DBT/NDRL//2019/09). The collected plant samples were used to isolate endophytes.

209

210 **2.2. Isolation of fungus from leaves**

211 Fresh and healthy leaves (3-month-old, size-5cm long) of *T. connaroides* were collected and
212 washed thoroughly in distilled water, following the method described by Talukdar et al., (2021).
213 Surface sterilizing (ethanol) of leaves is commonly used in microbiology and plant science prior
214 conducting studies to eliminate surface pollutants such as fungus, bacteria, and other microbes.
215 Subsequently, the surface of each leaf was sterilized with ethanol 70% for 1 min, then a mixture of
216 sodium hypochlorite (to 2%) for 30 min, and again rinsed with ethanol 70% for 30 s. For using
217 sodium hypochlorite to remove any remaining bleach, rinse the leaves several times with sterile
218 distilled water. After that, the leaves were washed three times with sterile distilled water. After surface
219 sterilization, the plant material was dried on sterile blotting paper, and a manual method was used to
220 prepare potato dextrose agar (PDA) (Hi-Media, Mumbai, PDA) medium containing the antibiotic
221 chloramphenicol (at 0.02%). The leaves were chopped to expose the inner surface of the plant (0.5
222 mm in diameter), placed on a PDA plate, and incubated at $27 \pm 2^\circ\text{C}$ for 6 to 7 days. Every day for
223 monitoring on the development of mycelia. Hyphal tips that were emerging from the leaf sections
224 were put on PDA slants, sub cultured, and kept at 4°C (Tolulope et al., 2015). Inoculated plates were
225 incubated in the biological oxygen demand (B.O.D) at temperature $27 \pm 2^\circ\text{C}$ for up to 7 days to
226 further analysis (Santra et al., 2022).

227

228 **2.3. Morphology identification of *Trichilia connaroides*-4 (TC-4) fungus**

229 The colony and spore's morphological features were examined to determine the TC-4 isolate.
230 According to recognized identification guidelines, the isolates were identified based on their
231 morphological and microscopic features (Cara et al., 2022; Zabouri et al., 2022). The purification
232 procedures used a 5-day-old endophytic fungal culture to evaluate fungi morphology (Ismail et al.,
233 2017). The PDA medium was employed for the morphological findings observe their colony surface,
234 granular, powdery, mountainous, growth area, and concentric stripes (Sangeetha & Ashtaputre, 2015).
235 A microscope with a $100\times$ magnification was employed for the microscopic examination

236 (Lactophenol cotton blue stain (LPCB), Hi-Media, Mumbai) (Manan et al., 2017; Ranganathan &
237 Mahalingam, 2019).

238

239 **2.4. DNA extraction and polymerase chain reaction (PCR) amplification**

240 Fungal isolates were grown from single conidia and verified by sequencing that the internal
241 transcribed spacer (ITS) region was amplified using the universal primers ITS1 and ITS4 region of
242 the ribosomal DNA. The isolates were grown on PDA for seven days at 28°C for DNA extraction.
243 The mycelia were extracted, lyophilized, and then frozen in liquid nitrogen. The genomic DNA was
244 extracted, according to Suneja et al. (2023). The NanoDrop spectrophotometer 2000 (Thermo
245 Scientific) was used to measure the quantity and quality of the genomic DNA at 260 and 280 nm
246 before the following step.

247 After that, the ITS region of the isolated DNA was amplified using a PCR (Khalil et al., 2021).
248 Two ITS primers were used, i.e., ITS Primer Forward: 5'TCCGTAGGTGAACCTGCCG3' and
249 Reverse Primer: 5' TCCTCCGCTTATTGATATGC 3'. The following were used in the
250 amplification of 25 µL: dNTP to 0.2 mM, DreamTaq 1x buffer (including MgCl₂), ITS1 and ITS4
251 primers to 0.5 pmol, Taq polymerase to 0.125 U, 100 ng of DNA template, and 5.75 µL of NFW.
252 Pre-denaturation at 95°C for 5 min was followed by 35 cycles of denaturation at 95°C for 15 s,
253 annealing at 57°C for 15 s, and extension at 72°C for 45 s during DNA amplification. After 5 min of
254 post-extension at 72°C and 5 min of chilling at 4°C, the PCR process was completed. The PCR
255 products were observed by electrophoresis on 1% agarose gel dissolved in Tris acetate EDTA (TAE)
256 solution. TAE buffer was used for the electrophoresis. First, 2 µL of the DNA sample and 2 µL of
257 loading dye were mixed, and the mixture was then loaded into the agarose gel well. A 4 µL, 1.5 Kb
258 ladder was then placed into one of the gel wells to serve as a marker well once introduced. A voltage
259 of 110V was used to electrophorese the samples for 30 min. The gel was then immersed in ethidium
260 bromide (EtBr) solution for 30 min, followed by a 5-min wash with distilled water. Finally, a UV
261 transilluminator was used to view the electrophoresis products, like Kusumaningrum et al. (2014).
262 Subsequently, the amplified region was purified and sequenced using the QIA Rapid PCR
263 Purification Kit (QIAGEN). Endophyte ITS sequences were compared to a database cataloged in
264 NCBI using BLAST, and phylogenetic relationships were performed by the CLUSTAL X software
265 (Venkateswarulu et al., 2018). The 5.8S rDNA nucleotide sequence was edited with BioEdit software
266 and aligned with CLUSTALW 2.0 software (Hall, 1999). Fourteen sequences were used in a
267 phylogenetic analysis using the neighbor-joining method with 1,000 bootstrap replications based on
268 the Kimura 2-parameter test of the MEGA 6.0 software, according to Tamura et al. (2011).

269

270 **2.5. Extraction of secondary metabolites**

271 *A. macrospora* was scale cultivated in a 1000 mL Erlenmeyer flask with 500 mL of PDB. The
272 glass flasks were incubated for 15 days at pH 7.0 and 27 °C, which are the ideal conditions for growth.
273 By using Whatman No. 1 filter paper and washing the fungus mycelial mat more than five times in
274 distilled water, unfavorable broth components have been extracted from the medium. Mycelium was
275 combined with ethyl acetate (500 mL) and transferred to 1000 mL glass beakers containing fungus
276 mat (100 g) for cold extraction for 20 days at 27 °C ±2 °C. After full extraction, Whatman No. 1 filter
277 paper was used to separate the liquid component from the mycelium. The metabolites were obtained
278 by evaporating the solvent using a rotary vacuum evaporator (Hei-VAP series, Heidolph Instruments)
279 at low temperature (40°C-50°C) and reduced pressure after filtration with sterilized cotton filter and
280 Whatman no.1 filter paper, like Ragavendran et al. (2017) and Mahmud et al. (2020).

281

282 **2.6. Collection of mosquitoes**

283 At the developmental stage, the first to fourth instar larvae, pupae, and eggs of *A. aegypti* were
284 collected from the Indian Council of Medical Research-Centre for Research in Medical Entomology
285 in Madurai, Tamil Nadu, India. The collected larvae, pupae, and eggs were maintained in deionized
286 water at 25 ± 2°C with a photoperiod of 10/14 h day/night. The food contains pedigree biscuits,
287 sucrose, and brewing yeast in a 4:1:1 ratio and is kept at room temperature for 24 h before the start of
288 the experiment, according to WHO (2005).

289 **2.7. 4th instar larvae of the *A. aegypti* metabolite (500µg/mL) based behavioral study**

290 In a larvicidal bioassay, the larvae were closely examined for behavioural alterations (n=300/groups),
291 such as increased wiggling movement, vertical and horizontal activity, and self-biting behaviors. Using
292 a Nikon D-SLR digital camera (Nikon Inc., Japan), indications of larval behaviour were noted and
293 captured on camera. In a similar manner, control as well as treated larvae were both recorded and
294 compared (da Silva et al., 2013).

295

296 **2.8. Larvicidal and pupicidal bioassays**

297 The experiments, including larval (1st - 4th instars) and pupal stages, were used for larvicidal and
298 pupicidal bioassays according to WHO (1981) protocol with minor modifications. Briefly, fungal
299 metabolites (at 100, 200, 300, 400, and 500 µg/mL) were prepared. Each test larvae and pupae were
300 placed in a 200 mL beaker filled with distilled water. The test solution was dissolved in 1 mL of
301 dimethyl sulfoxide (10% DMSO) and tested against 1st to 4th instar larvae and pupae. The number of
302 dead larvae was counted in 24 h and pupae in 48 h, and the mortality rate was calculated using
303 Abbott's formula (1925) (Equations 1 and 2). A negative control group (10% with distilled water, no

304 addition of fungal metabolites) was included in each bioassay, and for each concentration, we
305 performed tests five times.

306

$$307 \quad \text{Corrected mortality} = \frac{(\text{Observed mortality in treatment} - \text{Observed mortality in control})}{100 - \text{Control mortality}} \times 100$$

308

Eq. 1

309

$$310 \quad \% \text{ mortality} = \frac{\text{Number of dead larvae}}{\text{Number of larvae introduced}} \times 100 \quad \text{Eq. 2}$$

311

312 2.9. Ovicidal bioassay

313 The ovicidal activity was determined by measuring the inhibition of egg hatchability. *A. aegypti*
314 oocytes collected from laboratory colonies were cultured in room conditions at $27 \pm 2^\circ\text{C}$. The newly
315 laid eggs were observed with a stereomicroscope to evaluate the survival rate. Approximately 30 viable
316 eggs were collected and exposed to various concentrations (range 100 to $500\mu\text{g/mL}$) of mycelial
317 metabolites. The test was repeated five times, and the negative controls were kept separately. Results
318 were recorded by observing egg hatchability 72 h after treatment (Pineda-Cortel et al., 2019; Deepak
319 et al., 2019). Abbott's formula was used to correct the control's zero mortality (Abbott, 1925)
320 (Equation 3).

321

$$322 \quad \text{Ovicidal activity} = \frac{\text{Number of unhatched eggs}}{\text{Total number of eggs introduced}} \times 100 \quad \text{Eq. 3}$$

323

324 2.10. Acetylcholinesterase assay

325 To evaluate the possible cholinesterasic effect of the treatments, the total body homogenates
326 of 50th 4th instar *A. aegypti* larvae (100 μL) were spectrophotometrically examined using the Ellman
327 and others (1961) procedure with acetylcholine iodide as a substrate (Dahran et al., 2023). *A.*
328 *aegypti* 4th -instar larvae for testing were extracted with a dropper container at first. Deionized water
329 was used to wash the larvae twice, and filter paper was used to wipe the water off their surfaces.
330 Second, a 1.5 mL centrifuge tube was used to hold the larvae. A crushing rod was then used to mill
331 0.6 mL of ice-cold, 0.1 M PBS buffer (pH 8.0) in an ice bath for 30 s. Third, using an ultrasonic
332 crusher, the larvae were subjected to ultrasound 20 times at an ambient temperature. In order to
333 remove the remaining pieces of larval tissue, the tube was centrifuged at 4000 rpm for 15 min at 4°C ,
334 and the supernatant was collected to produce the AchE solution that would be evaluated. To
335 determine the total AChE activity in the presence or absence of the mass per unit volume inhibitor,

336 the concentration of AChE was carried out in two distinct 96-well plates. 25 μ L of homogenates were
337 added to 145 μ L of Triton/Na phosphate (5 μ L of 100% Triton X-100 in 50 μ L of 1M sodium
338 phosphate buffer at pH 7.8 and 455 μ L of distilled water) and 10 μ L of DTNB/Na phosphate (10
339 mM DTNB in 100 mM sodium phosphate buffer at pH 7.0) and kept in triplicates. All plates were
340 placed at room temperature, with light protection, and spectrophotometric scans for 1 h (at 405 nm).
341

$$\text{AChE activity inhibition (\%)} = \frac{(\text{Acontrol} - \text{Asample})/\text{Acontrol}}{\text{Acontrol} - \text{Asample} = \text{O. D of control sample}} \times 100$$

342
343

344 2.11. Histopathological study

345 A histopathological analysis of a mosquito sample was performed to detect possible changes in
346 morphological characteristics induced by the reaction of fungal metabolites. The test mosquito's 4th
347 instar larvae (n=20/group) were treated with a metabolite treatment, while the control and treated
348 larvae were fixed with 10% formalin. The tissues were then fixed in paraplast, sectioned (5 μ m thick),
349 and dehydrated using an ethyl alcohol series before being cleaned in xylene. Hematoxylin and eosin
350 (H&E staining) were done using the usual section staining method, like Khalifa et al. (2022). Finally, a
351 Labomed light microscope (LX-200) was used to study the midgut region of control and treated
352 larvae (at a magnification of around 40 \times), and images were taken (Yamany et al., 2022).

353

354 2.12. Antibacterial activity

355 The bacterial strains *Bacillus subtilis* (MTCC 441), *Staphylococcus aureus* (ATCC 25923),
356 *Escherichia coli* (ATCC 25922), and *Salmonella typhi* (MTCC 98) were obtained from the
357 Department of Microbiology at Mohan Kumaramangalam Medical College in Salem, Tamil Nadu,
358 India (Natarajan et al., 2014). All isolates were maintained on a nutrient agar medium (NA). The
359 antibacterial activity of the extracted bioactive metabolites was evaluated by agar well diffusion
360 method, like Maliehe et al. (2022). Each bacterial strain was swabbed evenly onto the individual plates
361 using sterilized cotton swabs. On Mueller Hinton agar (MHA, Hi-Media, Mumbai) plates, 6 mm-
362 diameter wells were produced using gel puncture, and four concentrations (25, 50, 75, and 100
363 μ g/mL) of fungal mycelium metabolites were loaded on the well. The plates were not disturbed for 1
364 h to achieve uniform diffusion of substances into the agar. The plates were incubated for 24 h at 37 $^{\circ}$ C.
365 Using an antibiotic zone scale, the diameter of the inhibition zone around the wells was measured and
366 calculated in millimeters (mm). Negative (10% DMSO to 20 μ L, v/v) and positive control
367 (ciprofloxacin to 4 μ g/mL). Negative growth zones were only assessed after 24 h to prevent false
368 findings. Each experiment was performed three times, like Sharma et al. (2016).

369

370 **2.13. Cytotoxicity effects on human cervical cancer cells**

371 HeLa (human cervical cancer) cell strain was obtained from National Centre for Cell Sciences
372 (NCCS) (Pune University, India) and grown in the Eagle's minimal essential medium (EMEM)
373 containing 10% of fetal bovine serum (FBS). Cell cultures were maintained weekly at 5% CO₂, 37°C,
374 95% air, and 100% relative humidity (RH), and the medium was replenished twice every seven days.
375 Monolayer cells were exfoliated with trypsin-EDTA to prepare a single-cell suspension, and the viable
376 cells were counted on a hemacytometer. The medium was diluted to a final density of 1×10^5
377 cells/mL using FBS to 5%. After seeding 100 μ L of cell suspension per well in 96-well plates with a
378 plating density of 10,000 cells/well, the plates were incubated at 37°C, 5% CO₂, 95% air, and 100%
379 RH for cell adhesion. After 24 h, the cells were treated with various concentrations of the mycelial
380 extract. First, they were dissolved in neat DMSO (10%), then diluting the sample aliquots in serum-
381 free medium to twice the desired maximum concentration. Additionally, serial dilutions of up to 4-
382 fold were performed for five concentrations. Aliquots (100 μ L) of these variable dilutions were added
383 to the appropriate wells containing 100 μ L medium, and the final concentrations required were
384 totaled. After adding the sample, the plates were incubated at 37°C, 5% CO₂, 95% air, and 100% RH
385 for two days. 10% DMSO should be included as control. The sample-free medium served as a
386 control. Chemical 3-[4, 5-Dimethylthiazole-2-yl] 2,5-diphenyltetrazolium bromide (MTT) cleaves the
387 tetrazolium ring with the enzyme succinate dehydrogenase and converts it to insoluble purple
388 formazan. The amount of formazan produced is directly proportional to the number of viable cells,
389 so the reaction was analyzed. After two days of incubation, MTT (15 μ L to 5 mg/mL) in phosphate-
390 buffered saline (PBS) (pH 7.4) was added to each well and incubated at 37°C for 4 h. The formed
391 formazan crystals were solubilized in 100 μ L DMSO (100%), and the absorbance was measured at
392 570 nm. Cell viability was calculated using the following formula (Equation 4):

393

$$394 \text{ Viability \%} = \frac{\text{Test OD} - \text{Control OD}}{100}$$

Eq. 4

395

396 **2.14. Gas chromatography and mass spectroscopy (GC-MS) analysis**

397 The GC-MS analysis of fungal mycelial metabolites was performed in electron ionization (EI)
398 mode on GC-MS Perkin Elmer model 680 system (Switzerland). The initial temperature was set up
399 at 70°C for 2 min; oven temperature at 280°C (at the rate of an increase of 5°C/min) was maintained
400 for 9 min. The following were the GC-MS technique operating conditions: TR 5-MS standard non-
401 polar capillary column, 30 Mts, 0.25 mm ID, 0.25 μ m Film thickness. The mobile phase flow rate
402 (carrier gas: Helium) was fixed at 1.0 mL/min. The temperature program (oven temperature) for the

403 gas chromatography portion was 40°C elevated to 250°C at 5°C/min. The ionization voltage was kept
404 at 70 eV, and the samples were injected (1µL) in split mode (10:1). The mass spectrum was obtained
405 from 40 to 1000 a.m.u, like Ragavendran & Natarajan (2015). The compounds were identified by
406 comparing their retention time (RT) and mass spectrum using NIST-2008 library database
407 TurboMass ver. 5.8.9.

408

409 **2.15. Fourier-transformed infrared spectroscopy (FT-IR) analysis**

410 FT-IR spectroscopic studies were performed using an FT-IR (Shimadzu IR Affinity)
411 spectrophotometer with a scanning range of (4000-450 cm⁻¹). The disc was made by mixing potassium
412 bromide (KBr) with fungal mycelial metabolites in a 10:90 weight-to-volume ratio. Clean, dry nitrogen
413 gas was used to clean the detector, increasing the signal level, and removing moisture. The spectrum
414 was then measured once the discs were placed into the spectrophotometer. The online spectroscopic
415 analysis examined the FT-IR spectra, like Rajalakshmi & Mahesh (2014).

416

417 **2.16. Zebrafish embryo toxicity analysis**

418 The zebrafish embryo/larvae were exposed to different concentrations of mycelium extract
419 (250 µg/mL to 2 mg/mL) to evaluate its toxic range. The exposure period was calculated from 24
420 hours post fertilization (hpf) to 96 hpf. The survival rate was calculated as the total number of
421 embryos/larvae that survived during the exposure period. The malformation parameters such as
422 scoliosis, yolk sac edema (YSE), and bend tail (BT) were registered, like Malafaia et al. (2020). The
423 heart rate was recorded at 96 hpf and expressed as beat per min. The hatching rate was calculated at
424 the end of 48 hpf, according to Guru et al. (2023) and Priya et al. (2023). The experimental designs in
425 this research article were in accordance with ethical guidelines and approved by Periyar University -
426 Institutional Animal Ethics Committee (IAEC approval No.: PU-IAEC/2018/M1/04).

427

428 **2.17. *In-silico* toxicity prediction and Autodock studies**

429 The compound identified from the mycelium metabolites was investigated for the
430 computational toxicity analysis using ProTox-II online server (https://tox-new.charite.de/protox_II/).
431 Toxicity concentrations and toxicity classes for particular compounds can be predicted through this
432 tool. The molecular docking studies for the compounds with the target receptor (*Escherichia coli*
433 FimH protein and *Staphylococcus aureus* tyrosyl-RNA synthetase protein) was performed using the
434 Autodock software version 1.5.6. The targeted site of protein was downloaded from the protein data
435 bank (<https://www.rcsb.org/>). The amino acid interactions between the ligand and receptor were
436 visualized using the Discovery studio visualization (Velayutham et al., 2022).

437

438 2.18. Statistical analysis

439 Data were analyzed using SPSS statistical software (20.0 version). The LC_{50} and LC_{90} values
440 were calculated by Probit analysis with their lower and upper confidence levels (LCL and UCL). The
441 level of significance (p-value) was fixed at $p \leq 0.05$. Probit analysis was used to calculate the median
442 (LC_{50}) and maximum (LC_{90}) lethal concentrations (LCs) limits from this data (Finney, 1971).

443

444

445 3. RESULTS

446 3.1. Morphology identification of endophytic fungi from *T. connaroides* leaves

447 The seven-day old isolates of *Alternaria* culture grown on PDA plates were used to study the
448 morphological characters. The colonies of *A. macrospora* were grayish green in color and white with
449 septal hyaline and branched mycelium, solitary, dark brown, straight or slightly curved, oval conidia,
450 with a long-tapered beak. *Alternaria* sp. is based on the colony's diameters and lactophenol cotton
451 blue stain endophytic fungus shown in Figure 1A. Molecular screening provided additional
452 confirmation of this at the 5.8s rDNA species level. According to Venkatesh and Darvin (2016), the
453 morphological features of *A. macrospora* produced results comparable to those of the present study.
454 Researchers reported that conidia measured between $43.4 \times 13.3 \mu m$ and had 1 to 8 transverse septa
455 (Saleem and El-Shahir, 2022).

456

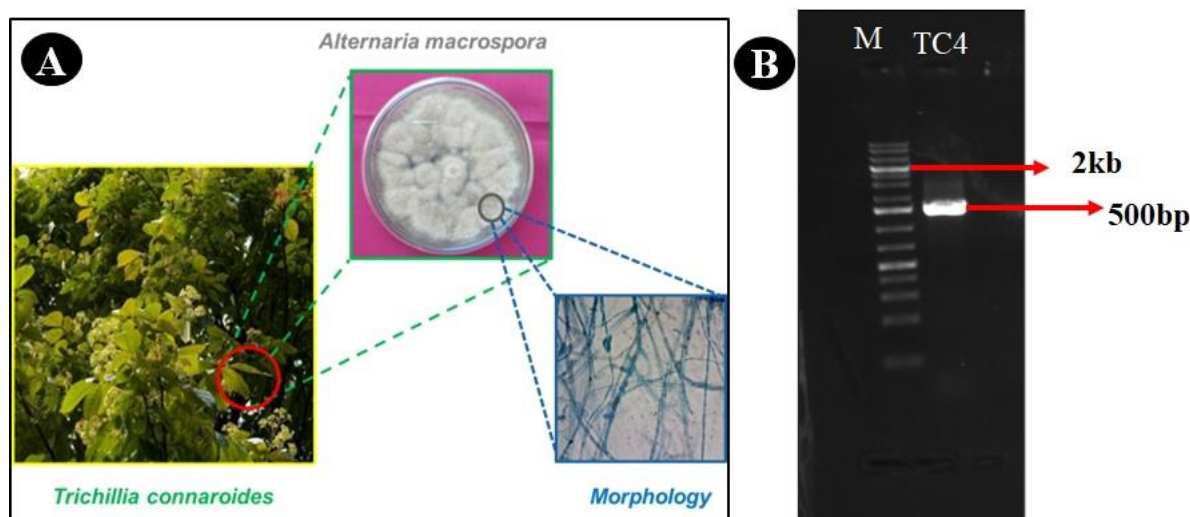


Figure 1. (A) Photography of the plant *Trichillia connaroides*, the fungal species *Alternaria macrospora* isolated and its microscopic view showing morphological characteristics. (B) PCR amplification of isolated genomic DNA at ITS regions (ITS 1 and ITS 4).

457

458 3.2. Molecular identification of isolated culture

459 The isolated DNA sample was amplified in optimized condition using the universal primer,
460 and the rDNA fragments were shown in Figure 1B. The obtained amplification product was located
461 in the expected ITS region with exactly 552 bp. The obtained RNA sequence of the isolated coding
462 5.8S rDNA gene was deposited in GenBank (NCBI), with accession number of MN049541.
463 Subsequently, based on 5.8S rDNA sequence analysis, the strain showed 99% similarity to the earlier
464 reported *Alternaria* sp. sequence. The phylogenetic tree analysis involved 15 fungal ITS sequences,
465 and phylogenetic tree analyzes were performed in MEGA 11. The ideal tree with the sum of the
466 length of the division = 1.99. The evolutionary history of the isolates interfered with the Neighbour-
467 Joining tree method is shown in Figure 2. The relationship between the taxa of the endophytic fungal
468 isolates and the reference taxa retrieved from GenBank has been shown. The percentage of replicate
469 trees in the bootstrap test (1000 repetitions) where the related taxa grouped were displayed above the
470 branches and the clades established were supported by bootstrap values >50%. The completed
471 database comprises 656 locations. MEGA 11 was used to perform evolutionary studies.

472

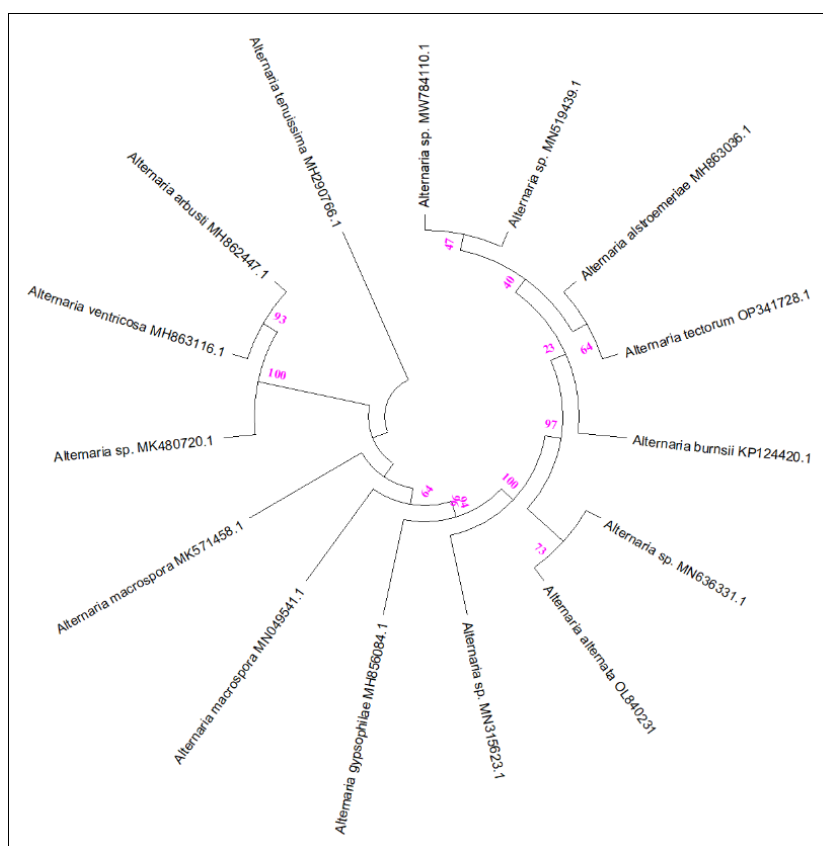


Figure 2. Phylogenetic tree analysis of *A. macrospora*. The percentage of replicates trees in which the associated taxa clustered together in the bootstrap test (1000

replicates) is observed next to the branches.

473

474 3.3. Larvicidal activity using endophytic fungi *A. macrospora*

475 Fungi and fungus-derived compounds are highly toxic to mosquitos but have low toxicity to
476 non-target organisms. Endophytic fungus *A. macrospora* mycelial metabolite was tested for larvicidal
477 activity against 1st - 4th instar larval stages of *Ae. aegypti*. The fungal metabolites exhibited superior
478 toxicity against 1st and 2nd instar larvae of *A. aegypti* after 24 h exposure and reported 99% larval
479 mortality. LC₅₀ values of 1st to 4th instar larvae were found to be “96.167, 131.370, 217.595, and
480 143.864 µg/mL” and “395.16, 483.62, 882.545 and 655.722 µg/mL” (Table 1). Also, the metabolite-
481 treated 1st and 2nd instar larvae revealed a distinct effect at the maximum concentration (500 µg/mL).
482 At the concentration of less than 200 µg/mL from *A. macrospora* mycelial metabolites, mortality rates
483 were slower, but larvae became very sluggish in movement compared to unexposed larvae (control).
484 More than 50% of larval deaths were observed within 8 h. Similarly, in the 3rd and 4th instar larvae, the
485 larval growth and development were arrested and affected. Among larval stages, concentration-
486 dependent growth inhibition was found to be in the order: 4th instar > 3rd instar > 2nd instar > 1st instar.

487 **Table 1.** Larvicidal and pupicidal effects of the *A. macrospora* mycelium metabolites against *A. aegypti*

Larva stages	Concentrations ($\mu\text{g/mL}$)	Mortality (%) \pm SD	LC ₅₀ ($\mu\text{g/mL}$) (LCL-UCL)	LC ₉₀ ($\mu\text{g/mL}$) (LCL-UCL)	χ^2	Significance
1 st instar	Control	0.0 \pm 0.0			4.976	0.970
	100	56.67 \pm 0.57				
	200	76.67 \pm 0.57	96.167	395.16		
	300	90.0 \pm 0.00	(46.786 -140.616)	(289.20 -635.091)		
	400	100.0 \pm 0.00				
	500	100.0 \pm 0.00				
2 nd instar	Control	0.0 \pm 0.0			7.973	0.951
	100	46.66 \pm 0.57				
	200	66.67 \pm 0.57	131.370	483.692		
	300	83.33 \pm 0.57	(80.182 -177.849)	(363.124 - 753.16)		
	400	100.0 \pm 0.00				
	500	100.0 \pm 0.00				
3 rd instar	Control	0.00 \pm 0.00			12.73	0.928
	100	36.66 \pm 0.57				
	200	53.3 \pm 0.57	217.595	882.545		
	300	76.67 \pm 0.57	(143.640 -288.134)	(622.50 - 1660.814)		
	400	93.3 \pm 0.57				

	500	100.0±0.00				
	Control	0.00±0.00				
4 th instar	100	40.0±0.47				
	200	56.67±0.55	143.864	655.722		
	300	73.3±0.57	(82.494 - 199.248)	(471.998 -1154.365)	10.24	0.936
	400	96.67±0.57				
	500	100.0±0.00				
	Control	0.00±0.00				
Pupae	100	33.3±0.57	234.390			
	200	46.67±0.47		739.362		
	300	56.67±0.00	(165.957 - 301.777)	(547.803-1222.998)	14.381	0.954
	400	100.0±0.00				
	500	100.0±0.00				

488 **Note** - LC₅₀: lethal concentration required to kill 50% of the population exposed, LC₉₀: lethal concentration required to kill 90% of the population
489 exposed larvae, χ^2 = chi square and SD: standard deviation.

490 **3.4. Pupicidal and ovicidal activity**

491 In pupicidal activity, the percentage of mortality was calculated at different
 492 concentrations of mycelia extracts from the endophytic fungus *A. macrospora* against *A.*
 493 *aegypti* (Table 1). The observed LC₅₀ and LC₉₀ values were 234.390 and 739.362 µg/mL,
 494 respectively. The mortality rate was calculated within the first 5 h of exposure, which
 495 exhibited 60% mortality. A 100% mortality in the pupae was reported after 48 h. The χ^2
 496 value was significant at $p \leq 0.05$ level. Table 2 shows the percentage of egg hatchability of
 497 *A. aegypti* subjected to five different dosages of an *A. macrospora* mycelia metabolite.
 498 This exposure had an ovicidal effect, indicating that it affected the capacity of mosquito
 499 eggs to develop. The table most likely depicts the metabolite's efficiency in inhibiting the
 500 hatching of *A. aegypti* eggs at various doses. The results can be displayed as a dose-
 501 response relationship, showing exactly the concentration of the metabolite interacts with
 502 the reduction in egg hatchability. No hatchability (100% mortality) was recorded at 500
 503 µg/mL compared to the control group (hatchability rate 96.8 to 100%). Also, LC₅₀ and
 504 LC₉₀ values were calculated as 36.080 and 204.422 µg/mL, respectively.

505

506 **Table 2.** Ovicidal activity of *A. macrospora* endophytic mycelium metabolites against *A.*
 507 *aegypti* eggs.

Concentrations (µg/mL)	Hatchability (%) ± SD	LC ₅₀ (µg/mL) (LCL-UCL)	LC ₉₀ (µg/mL) (LCL-UCL)	χ^2	Significance
Control	96.66±1.2				
100	73.33±0.00				
200	56.66±0.00	36.080	204.422		
300	43.33±0.57	(2.390 -	(110.541-	4.422	0.986
400	23.33±0.57	77.706)	355.100)		
500	NH				

508 **Note** - NH: no hatchability, LC₅₀: lethal concentration required to kill 50% of the
 509 population exposed, LC₉₀: lethal concentration required to kill 90% of the population
 510 exposed larvae, χ^2 = chi square and SD: standard deviation.

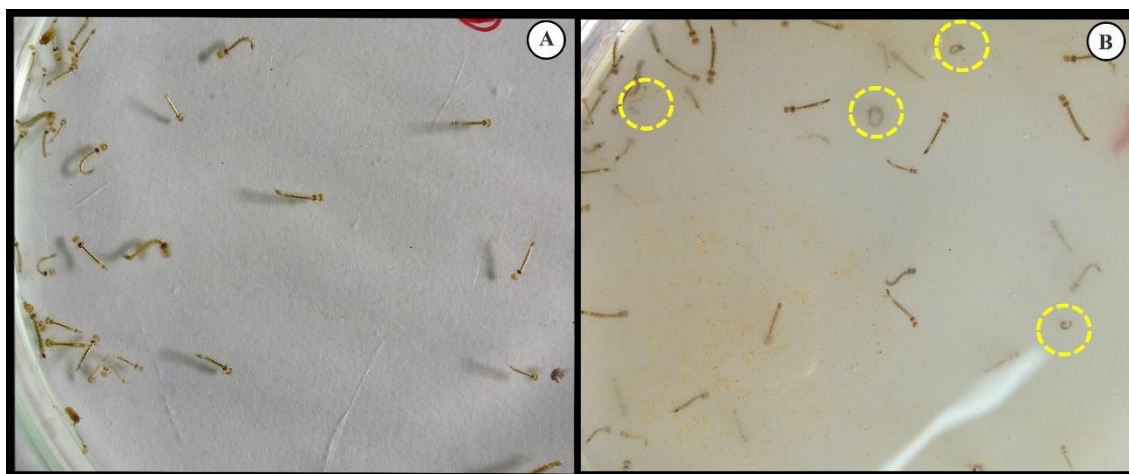
511

512 **3.5. Behavioural studies**

513 The *A. macrospora* metabolites induced behavioral toxicity on the 4th instar larval
 514 stage of *A. aegypti*. The control larval set showed normal behavior in contrast to the

515 vigorous and restless movement of larvae noticed after 25 min exposure to metabolites.
516 With increased exposure time, the larvae exhibited altered movements, abnormal
517 excitation and restlessness, and forceful self-nibbling of mouthparts and anal papillae,
518 leading to ring-shaped structures. Several larvae exhibited up-down wriggling movements,
519 vibrating movements, and paralytic symptoms (Figure 3).

520
521



522
523

524 **Figure 3.** Effectiveness of an ethyl acetate extract of *A. macrospora* as a larvicidal agent
525 against *A. aegypti* after 24 h of exposure. A). Larvae in control; B). Treated larvae (500
526 µg/mL). Self-biting larvae are indicated by a yellow circle.

527

528 3.5. Inhibition of AChE activity analysis

529 The AChE activity was significantly decreased at fungal mycelial metabolite
530 concentrations of 100 µg/mL, and the highest inhibition was noticed at 500 µg/mL. The
531 enzyme inhibition activity results clearly supported the metabolites' concentration-
532 dependent (Figure 4A). The direction at which the PROBIT plot for *A. macrospora*
533 slopes. The slope of the PROBIT plot is an important factor to consider into account
534 because it exhibits higher effects, i.e., maximum inhibition, at low concentrations, as
535 shown in Figure 4B, due to an elevated slope. However, the high linearity of the fit (r -
536 value= -0.986, $R^2 = 0.9721$ & p -value ≤ 0.0001) reflects a strong correlation in the
537 concentration dependent inhibition of AChE activity.

538

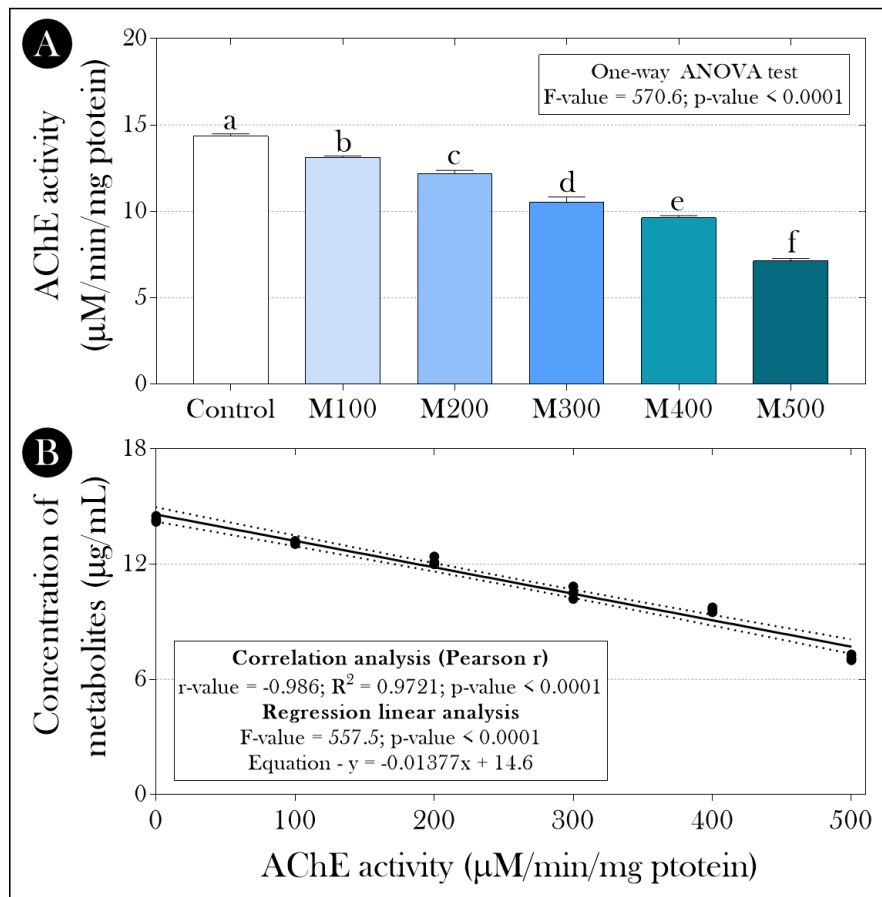


Figure 4. Acetylcholinesterase (AChE) activity in 4th instar *A. aegypti* larvae unexposed or exposed to different concentrations of the endophytic *A. macrospora* metabolites (M). (B) Linear correlation and linear regression analyze (concentrations of fungal metabolites vs. AChE activity). M100 to M500: groups of 4th instar *A. aegypti* larvae exposed to 100 to 500 µg/L of fungal metabolites. Parametric data are presented by the mean + standard deviation. Distinct lowercase letters indicate significant differences between experimental groups. The summaries of the statistical analyzes are displayed next to the graphs.

539

540 3.6. Histopathology analysis

541 The midgut architecture of *A. aegypti* larvae changed after exposure to the fungus
 542 mycelium metabolite. When larvae were exposed to mycelium metabolite, it resulted in
 543 the lysis of the midgut epithelium layer, vacuolization and significant destruction of the
 544 peritrophic membrane, loss, and degeneration of epithelial cells, gastrointestinal tract,
 545 midgut, cortex with hyperplasia of gut epithelial cells, ruptured brush border, damaged
 546 membranes, and microvilli (Figure 5B). Cellular organelles were severely affected even at
 547 a low dose (500µg/mL) treatment with *A. macrospora* metabolites. The control group, the

548 midgut of the *A. aegypti* larvae had a normal shape; the FB (food bolus), a single layer of
549 digestive cells with well-developed brush borders, epithelial layer, microvilli, cell
550 membranes, and cytoplasm areas in the midgut epithelium (Figure 5A).

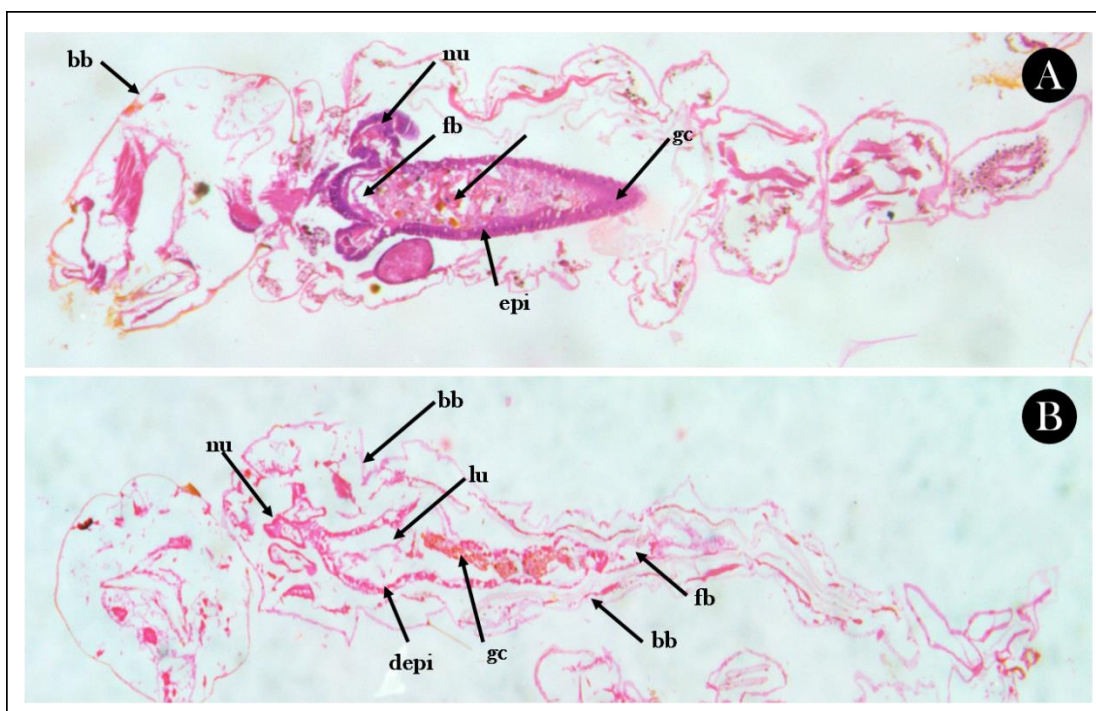


Figure 5. Histopathological profiles of control (A) and (B) 4th instar larvae of *A. aegypti* treated at 500µg/mL concentration of *A. macrospora* metabolite. bb: brush border; nu: nucleus; fb: food bolus; epi: epithelial cells; lu: lumen; depi: degenerative epithelial cells; gc: gastric caeca.

551

552 3.7. Antibacterial activity

553 The antibacterial activity of mycelium metabolites was evaluated against four
554 pathogenic bacterial strains, namely *S. aureus*, *E. coli*, *S. typhi*, and *B. subtilis*, with four
555 concentrations (25, 50, 75, and 100 µg/mL). Ciprofloxacin is a standard antibiotic to
556 compare the results with the zone obtained using mycelial metabolites. The maximum
557 inhibitory zone was observed in *E. coli* (22 mm), followed by *S. aureus* (20 mm), *B.*
558 *subtilis* (19 mm), and an average inhibition zone in *S. typhi* at 100 µg/mL (Figures 7A-E).
559 It shows that the antibacterial activity of mycelial metabolites strongly depends on the
560 concentration of mycelial metabolites present in the reaction mixture, as shown in Figure
561 6A-D. No inhibition zone was observed in the negative control (DMSO to 10%).

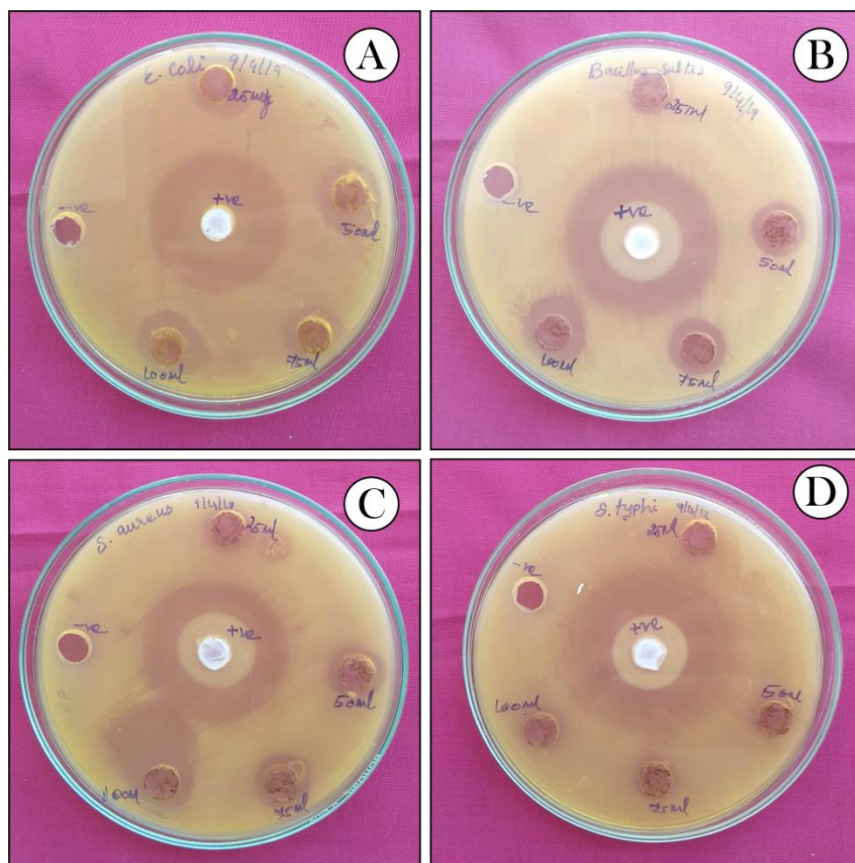


Figure 6. Antibacterial bioassay by agar well diffusion method. A) *E. coli*, B) *B. subtilis*, C) *S. aureus*, D) *S. typhi* zone of inhibition plates. -ve: negative control (only 10% DMSO); +ve: positive control (ciprofloxacin-4 µg/mL); Different concentration of *A. macrospora* metabolites loaded on four different well such as 25, 50, 75 and 100 µg/well.

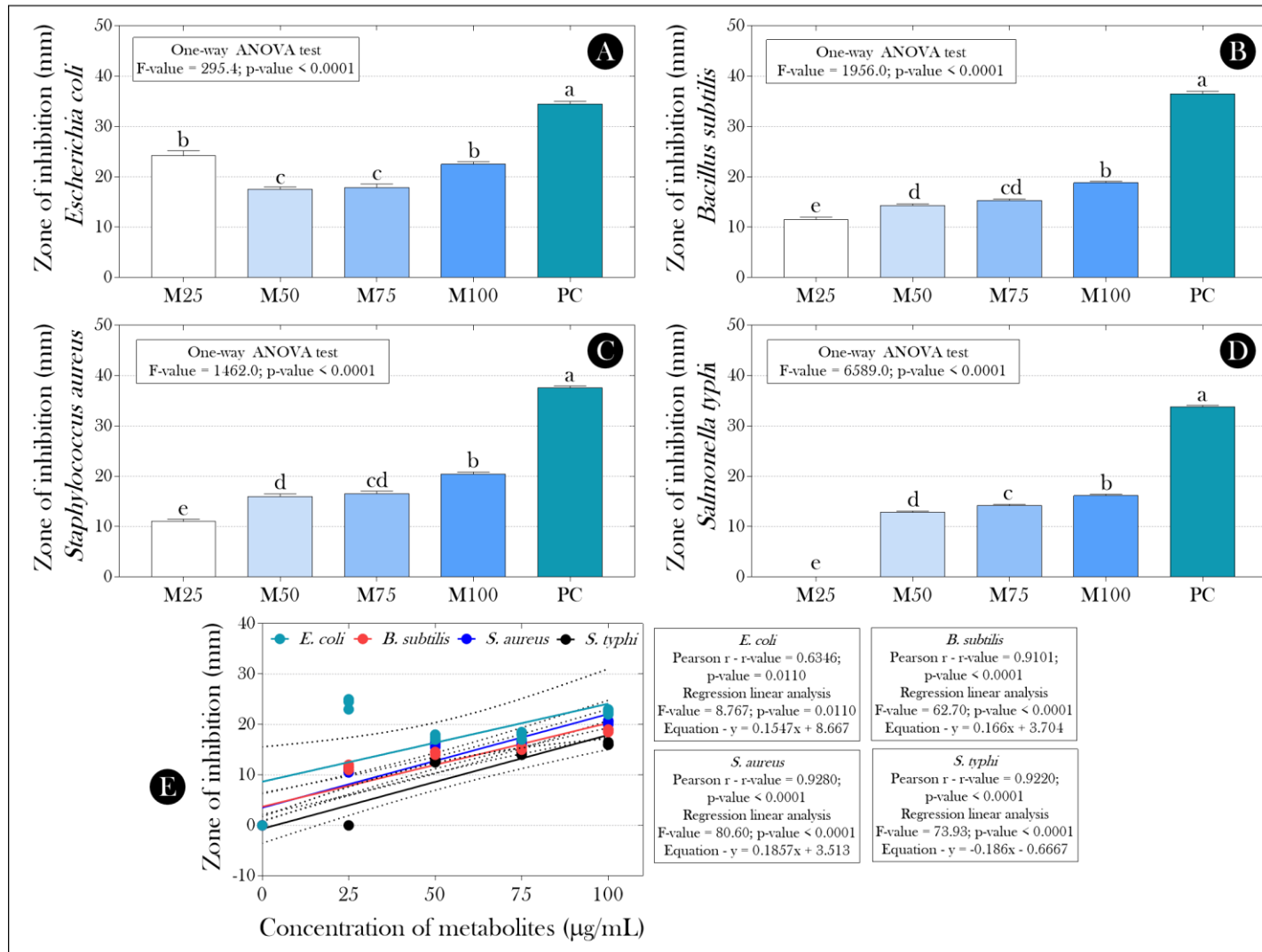


Figure 7. Antibacterial activity (zone of inhibition) of mycelium metabolites evaluated against (A) *Escherichia coli*, (B) *Bacillus subtilis*, (C) *Staphylococcus aureus*, and (D) *Salmonella typhi* exposed to four concentrations (25 to 100 µg/mL). (E) Correlation and linear regression analyze (concentrations of fungal metabolites vs. zone of inhibition). Parametric data are presented by the mean + standard deviation. Distinct lowercase letters indicate significant differences

between experimental groups. The summaries of the statistical analyzes are displayed next to the graphs.

563

564 3.8. Cytotoxic effects on HeLa cells

565 The cytotoxic activity of fungal endophytes was tested by MTT assay on the HeLa
566 cell line. Cells were exposed to variable concentrations of fungal metabolites (50-300
567 $\mu\text{g}/\text{mL}$), and changes in cell shape were observed under an inverted microscope. The IC_{50}
568 value of *A. macrospora* mycelial metabolites was 118.49 $\mu\text{g}/\text{mL}$. When the concentration
569 of mycelial metabolites was increased to 18.75, 37.75, 75, 150, and 300 $\mu\text{g}/\text{mL}$, the
570 percentage of cell inhibition was increased to 10.38 ± 1.5 , 21.64 ± 1.0 , 37.66 ± 0.5 , 56.27
571 ± 1.0 and $68.18 \pm 1.0\%$, after 24 h of incubation, evidencing a concentration-dependent
572 effect (Figure 8A-B). In the present work, the morphological alterations of the normal
573 cells were usually short and round. Still, the exposed cells exhibited noticeable
574 morphological changes like cell shrinkage, decreased cell volume, membrane blebbing,
575 loss of adhesion, and apoptotic body formation (Figure 8C-H).

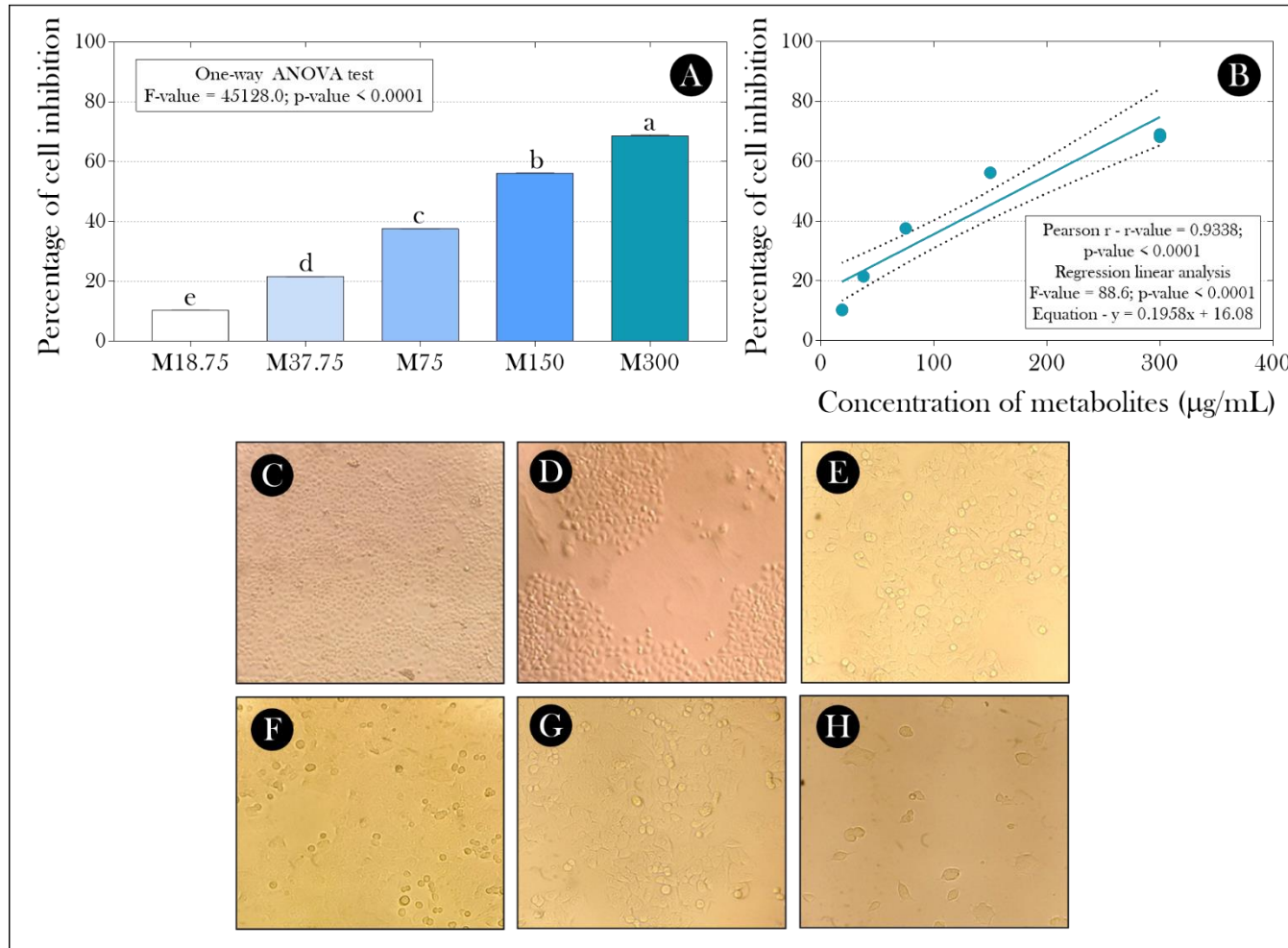


Figure 8. (A) Percentage of HeLa cell line inhibition exposed to different concentrations of the endophytic *A. macrospora* metabolites (M) (18.75 to 300 µg/mL). (B) Correlation and linear regression analyze (concentrations of fungal metabolites vs. percentage of HeLa cell line inhibition). Parametric data are presented by the mean + standard deviation. Distinct lowercase letters indicate significant differences between experimental groups. The summaries of the statistical analyzes are displayed next to the graphs. (C-H) Imagens representatives of the (C) HeLa control cell line

and exposed to mycelial metabolites to (D) 18.75 $\mu\text{g/mL}$, (E) 37.57 $\mu\text{g/mL}$, (F) 75 $\mu\text{g/mL}$, (G) 150 $\mu\text{g/mL}$ and (H) 300 $\mu\text{g/mL}$.

576 **3.9. GC-MS analysis**

577 GC-MS analysis of *A. macrospora* fungal metabolites produced some bioactive
578 compounds. The compounds were identified based on NIST databases by their
579 comparisons to actual mass spectral data (Figure 9A and Table 3). Here, a total of seven
580 compounds were identified: phenol, 3,5-bis(1,1-dimethylethyl) (4.572%), 3-isopropoxy-
581 1,1,1,7,7,7- hexamethyl-3,5,5-tris (trimethylsiloxy) tetrasiloxane (4.453%),
582 dihydroartemisinin, 10-o-(t-butyloxy (8.33%), cyclohexanol, 4-ethenyl-4-methyl-3-(1-
583 methylethenyl) (15.284%), oleic acid (22.093%), eicosanoic acid (9.407%), ether, 6-
584 bromo-1-ethyloctyl methyl. The chemical structure of these compounds is depicted in
585 Figure 9B.

586

587 **3.10. FT-IR analysis**

588 The FT-IR spectrum (4000-400/cm) of mycelial metabolites of *A. macrospora*
589 confirmed the presence of various functional groups of different organic compounds
590 (Figure 9C and Table 4). The sharp and strong spectrums indicated bands at 3317.54,
591 2924.09, and 2854.65 cm^{-1} were assigned to O-H and C-H stretching vibrations of
592 alcoholic, alkynes, and alkyl groups. The broad peak at 1710.86 cm^{-1} corresponds to the
593 C=O stretching of carboxylic acid present in the sample. The medium band at 1656.85
594 cm^{-1} can be described as C=C stretching vibration, indicating the presence of alkenes
595 groups. The strong band could be assigned at 1305.81 cm^{-1} , 1452.40 cm^{-1} corresponding to
596 C-H bend, and C-F stretch provides alkyl and halide groups. A peak at 1232.51 cm^{-1}
597 denotes the alkyl halides (C-F stretch). The absorption bands have exhibited the presence
598 of the ethers group at 1259.52 cm^{-1} (=C-O-C stretch). The peak at 1163.08 demonstrated
599 the presence of esters (O=C-O-C stretch). The medium peak at 1099.93 showed the
600 presence of alcohol (C-O stretch) groups. The strong 844.82 and 800.46 cm^{-1} peaks
601 indicate the alkyl halides (C-Cl stretch). A peak at 698.23 cm^{-1} revealed the alkenes (=C-H
602 bend).

603

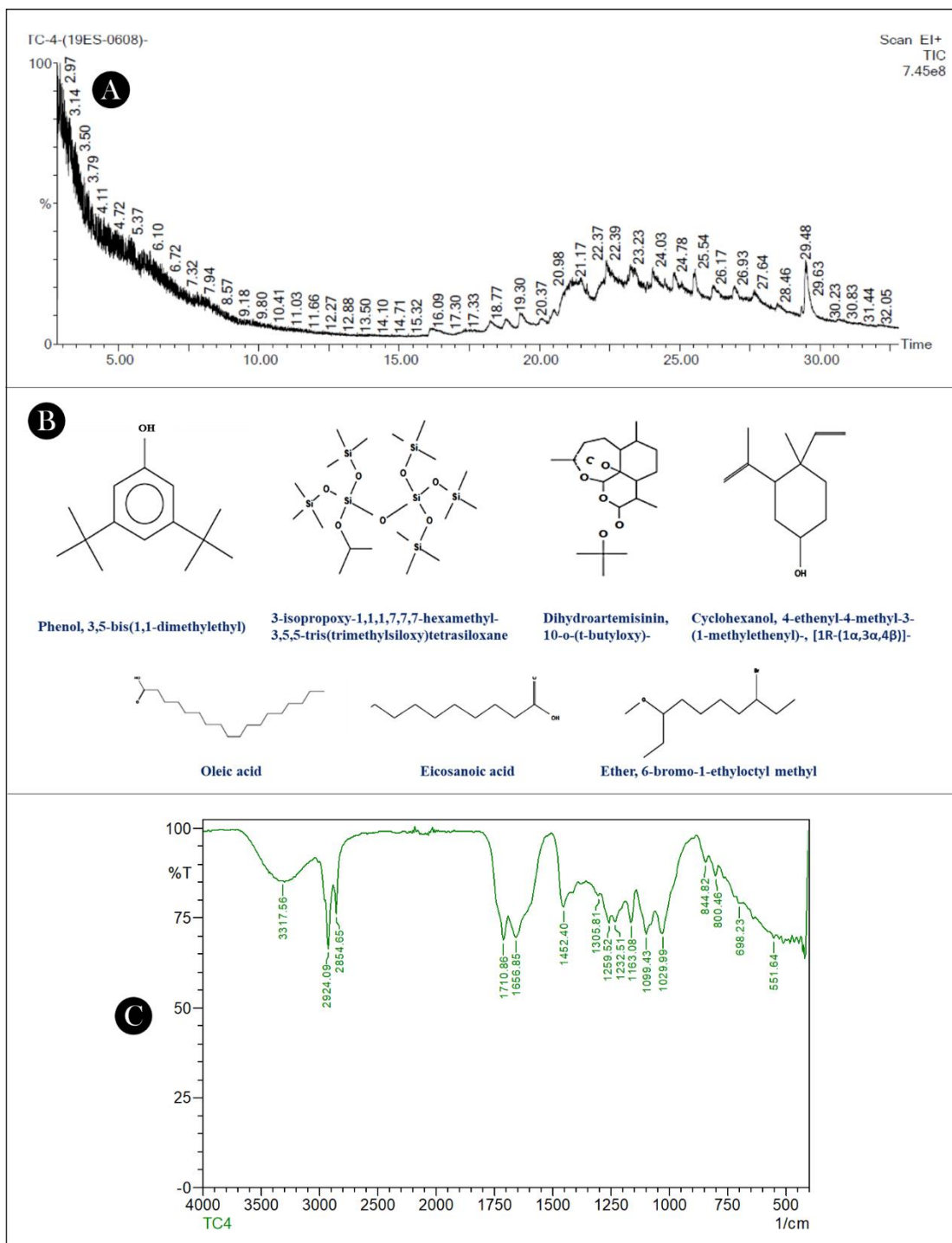


Figure 9. (A) Gas chromatography and mass spectroscopy (GC-MS) analysis, (B) chemical structures, and (C).Fourier-transformed infrared spectroscopy (FT-IR) spectrum of endophytic *A. macrospora* metabolites.

604 **Table 3.** Identification of secondary metabolites from ethyl acetate metabolites of *A. macrospora* by Gas chromatography and mass spectroscopy
 605 (GC-MS) analysis.

S. no	Compound names	R _r	Area (%)	Molecular formula	Molecular weight	Biological activity	References
1.	Phenol, 3,5-bis(1,1-dimethylethyl)	29.48	4.572	C ₁₄ H ₂₂ O	206	Antimicrobial activity	Fabio Granados et al., (2016)
2.	3-isopropoxy-1,1,1,7,7,7-hexamethyl-3,5,5-tris(trimethylsiloxy)tetrasiloxane	25.54	4.453	C ₁₈ H ₅₂ O ₇ Si ₇	76	Antimicrobial activity	Gupta et al., (2017)
3.	Dihydroartemisinin, 10-o-(t-butyloxy)-	26.93	1.794	C ₁₉ H ₃₂ O ₆	56	Anticancer activity	Chan et al., (2013)
4.	Cyclohexanol, 4-ethenyl-4-methyl-3-(1-methylethenyl)-, [1R-(1 α ,3 α ,4 β)]-	23.23	15.284	C ₁₂ H ₂₀ O	180	-	-
5.	Oleic acid	22.37	22.093	C ₁₈ H ₃₄ O ₂	282	Larvicidal & Antioxidant activities	Wei et al. (2016) and Fontana et al. (2013)
6.	Eicosanoic acid	21.17	9.047	C ₂₀ H ₄₀ O ₂	312	Larvicidal and Antioxidant activities	Silva et al., (2016)
7.	Ether, 6-bromo-1-ethyloctyl methyl	24.78	4.182	C ₁₁ H ₂₃ OBr	250	-	-

606

607

608 **Table 4.** Identification of functional groups from ethyl acetate metabolites of *A.*
 609 *macrospora* by Fourier-transformed infrared spectroscopy (FT-IR).

S. No	Wavenumbers (cm ⁻¹)	Vibration	Visible intensity	Functional groups
1	3317.54	O-H stretching	Sharp	Alcohols or phenols
2	2924.09	C-H stretching	Strong	Alkenes/Alkyls
3	2854.65	C-H stretching	Strong	Alkenes/Alkyls
4	1710.86	C=O stretching	Broad	Carboxylic acids
5	1656.85	C=C Stretching	Medium	Alkenes
6	1452.40	C-H Bend	Strong	Alkanes/Alkyls
7	1305.81	C-F Stretch	Strong	Alkyl/Halides
8	1259.52	=C-O-C Sym stretch	Medium	Ethers
9	1232.51	C-F Stretch	Strong	Alkyls/Halides
10	1163.08	O=C-O-C Stretch	Strong	Esters
11	1099.93	C-O Stretch	Medium	Alcohols
12	844.82	C-Cl Stretch	Strong	Alkyls Halides
13	698.23	=C-H Bend	Broad	Alkynes

610

611 3.11. Toxicity effect on zebrafish embryo/larvae

612 The zebrafish embryos/larvae were tested with different concentrations of
 613 mycelium extract. The concentrations from 250 µg/mL to 1 mg/mL were found to be
 614 non-toxic in most of the biomarkers evaluated (Figure 10). But the higher 2 mg/mL
 615 concentration was toxic (Figure 10). A significant difference in survival (63%), hatching
 616 (86%), and heartbeat rate (142 beats/min) was observed in the 2 mg/mL treatment group
 617 (Figure 10A-C, respectively). The malformation was observed in the 96 hpf larvae with
 618 YSE and BT in animals exposed to endophytic *A. macrospora* metabolites to 2 mg/mL
 619 (Figure 11).

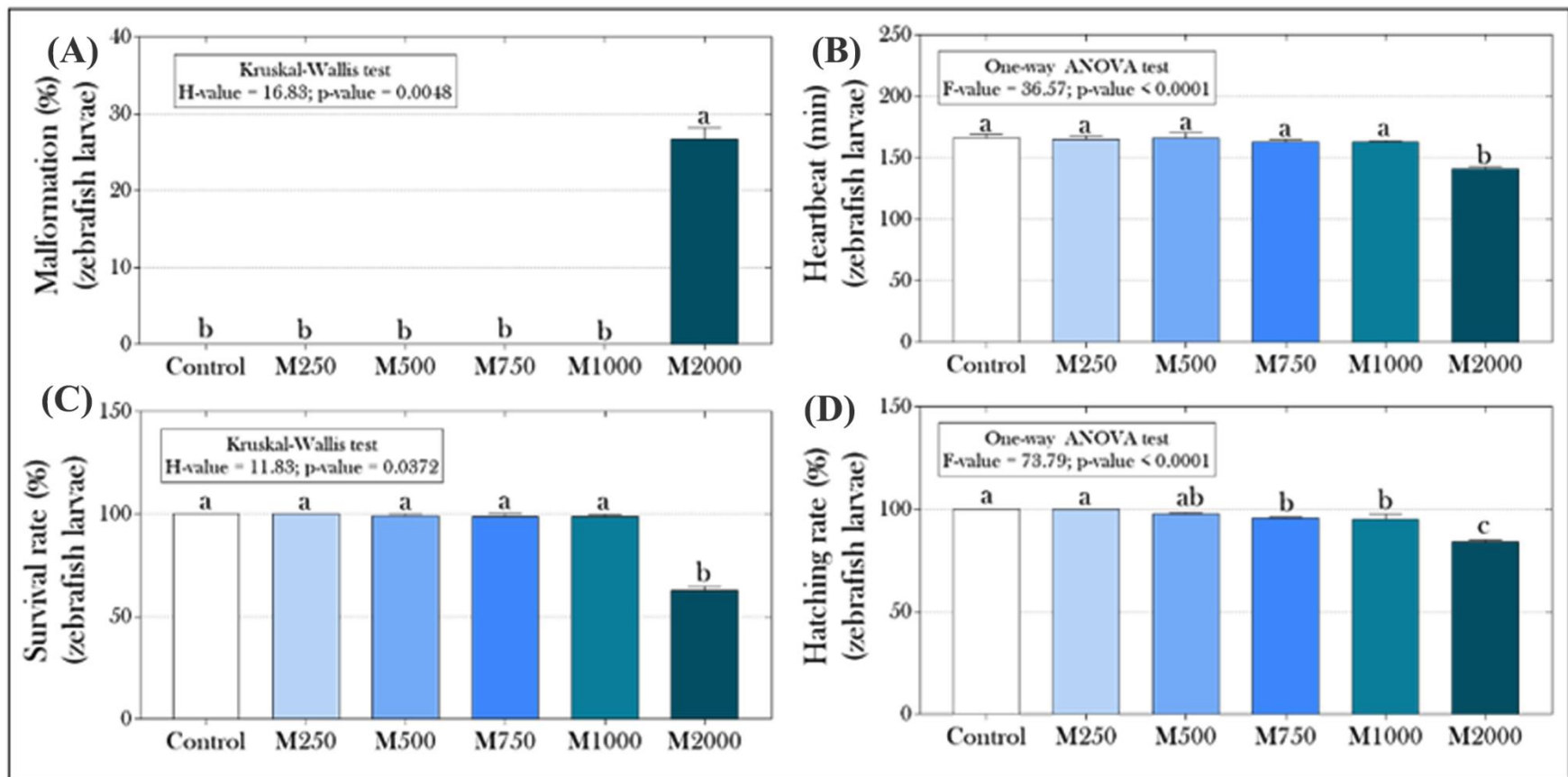


Figure 10. (A) Malformation rate (%), (B) heartbeat rate, (C) survival rate, and (D) hatching rate of zebrafish (*Danio rerio*) larvae unexposed or exposed to different concentrations of the endophytic *A. macrospora* metabolites (M) (250 to 2000 µL). Parametric data are presented by the mean + standard deviation, whereas non-parametric data are presented by the median and interquartile range. Distinct lowercase letters indicate

significant differences between experimental groups. The summaries of the statistical analyzes are displayed next to the graphs

620

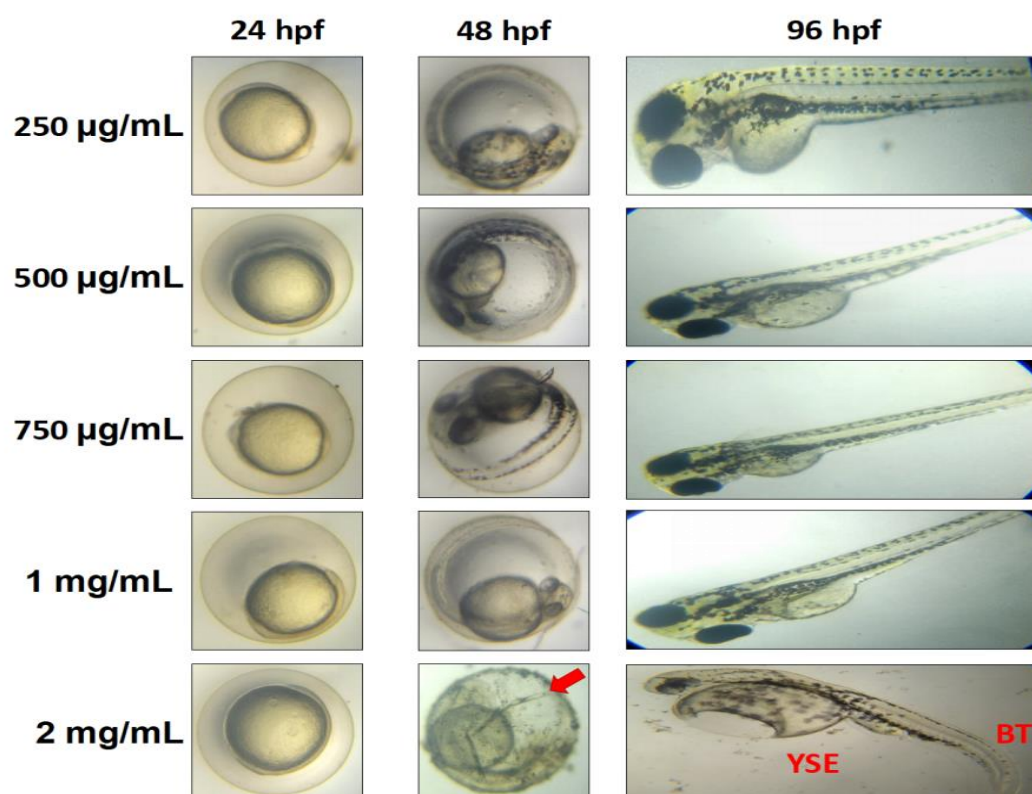


Figure 11. Representative images of eggs, embryos and larvae of zebrafish (*Danio rerio*) larvae exposed to different concentrations of the endophytic *A. macrospora* metabolites (M) (250 to 2000 μL) after 24, 48, and 96 hpf. YSE: yolk sac edema and BT: bend tail.

621

622 3.12. *In-silico* analysis of compounds on toxicity and binding affinity

623 The fungi metabolites identified from the GS-MS are investigated for toxicity
624 prediction. A decrease in toxicity class and LD50 (mg/kg) value indicates the toxic
625 condition of the compounds. In our study, the reported compounds have shown non-
626 toxic conditions except oleic acid. The oleic acid was less harmful, with a toxicity of class
627 2 and CL_{50} of 48 mg/mL (Table 5). The antibacterial potential of compounds can be
628 identified through their interaction ability with the pathogen receptor. Based on the
629 binding affinity value, the antimicrobial compounds are identified. In our results, the
630 fungi metabolites are docked with targets of *E. coli* FimH protein and *S. aureus* tyrosyl-
631 RNA synthetase protein. Among the metabolites, dihydroartemisinin, 10-o-(t-butyloxy)-
632 showed higher binding affinity in both the targets of *E. coli* FimH protein (-9.45 kcal/mol)
633 and *S. aureus* tyrosyl-RNA synthetase protein (-9.84 kcal/mol) (Figure 12A-G).
634 Dihydroartemisinin, 10-o-(t-butyloxy)- showed the amino acid interaction of TYR in *E.*

635 *coli* FimH protein and LYS, GLY, and ASP in *S. aureus* tyrosyl-RNA synthetase protein
636 (Table 6 & Figure 13A-G).
637

638 **Table 5.** *In-silico* analysis: toxicity profile of the compounds from ProTox online server

Compound	Predicted LD ₅₀ (mg/kg)	Predicted toxicity class	Water partition coefficient (logP)	Molecular refractivity	Topological polar surface area	Toxicity
Phenol, 3,5-bis(1,1-dimethylethyl)	965	4	18.24	255.86	65.57	Non-toxic
3-isopropoxy-1,1,1,7,7,7-hexamethyl-3,5,5-tris(trimethylsiloxy)tetrasiloxane	24134	6	6.56	151.36	54.61	Non-toxic
Dihydroartemisinin, 10-o-(t-butyloxy)-	567	4	3.94	91.62	55.38	Non-toxic
Cyclohexanol, 4-ethenyl-4-methyl-3-(1-methylethenyl)-, [1R-(1 α ,3 α ,4 β)]-	5300	5	4.75	70.42	0	Non-toxic
Oleic acid	48	2	6.11	89.94	37.3	Less toxic
Eicosanoic acid	900	4	7.11	100.03	37.3	Non-toxic
Ether, 6-bromo-1-ethyloctyl methyl	5000	5	4.15	63.95	9.23	Non-toxic

639

640

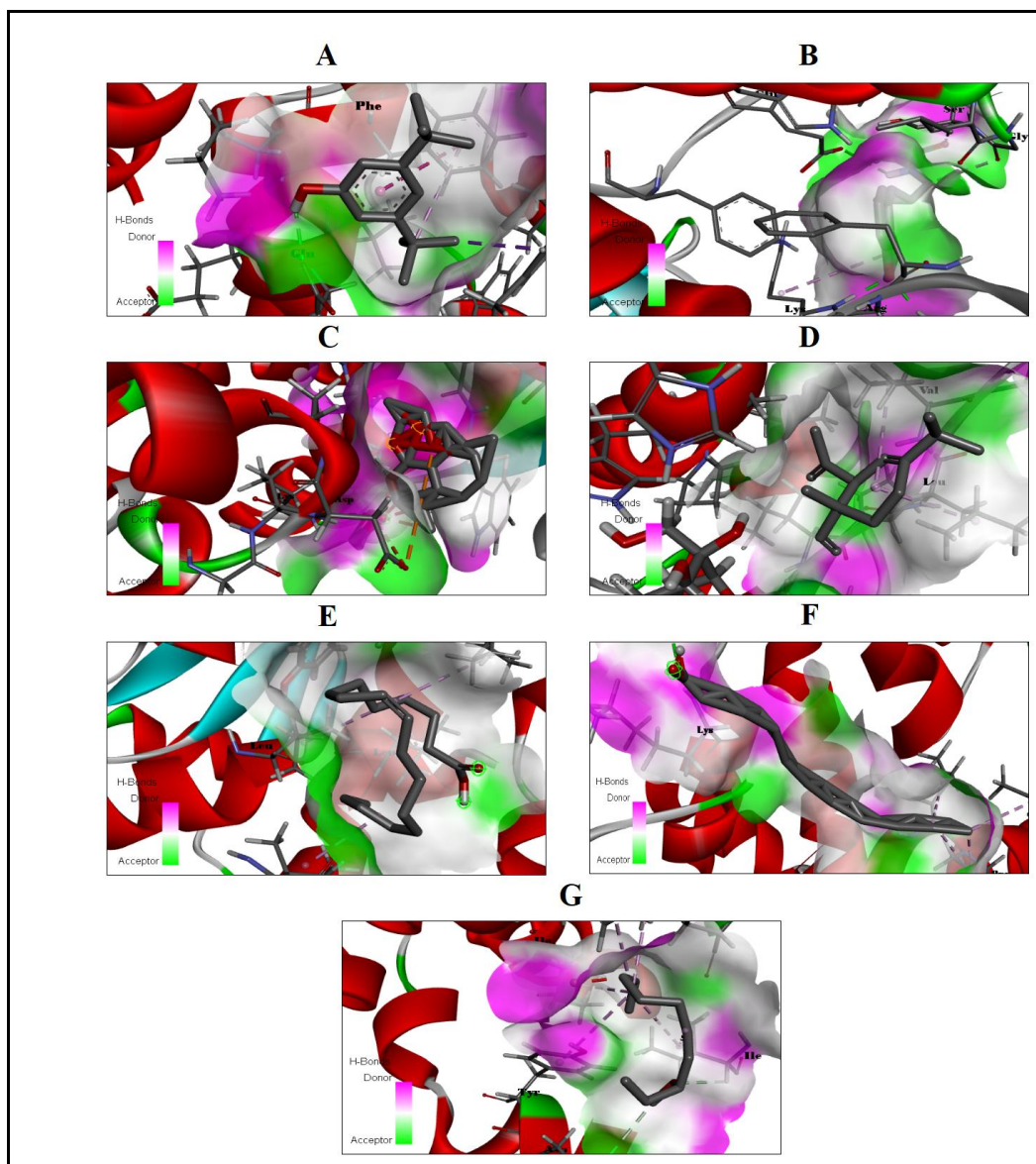


Figure 12. 3D interaction of different ligands with the targeted receptor of *Staphylococcus aureus* tyrosyl-RNA synthetase protein. (A) Phenol, 3,5-bis(1,1-dimethylethyl) (B) 3-isopropoxy-1,1,1,7,7,7-hexamethyl-3,5,5-tris(trimethylsiloxy)tetrasiloxane, (C) dihydroartemisinin, 10-o-(t-butyloxy)- (D) cyclohexanol, 4-ethenyl-4-methyl-3-(1-methylethenyl)-, [1R-(1 α ,3 α ,4 β)], (E) oleic acid, (F) eicosanoic acid, and (G) ether, 6-bromo-1-ethyloctyl.

642

643

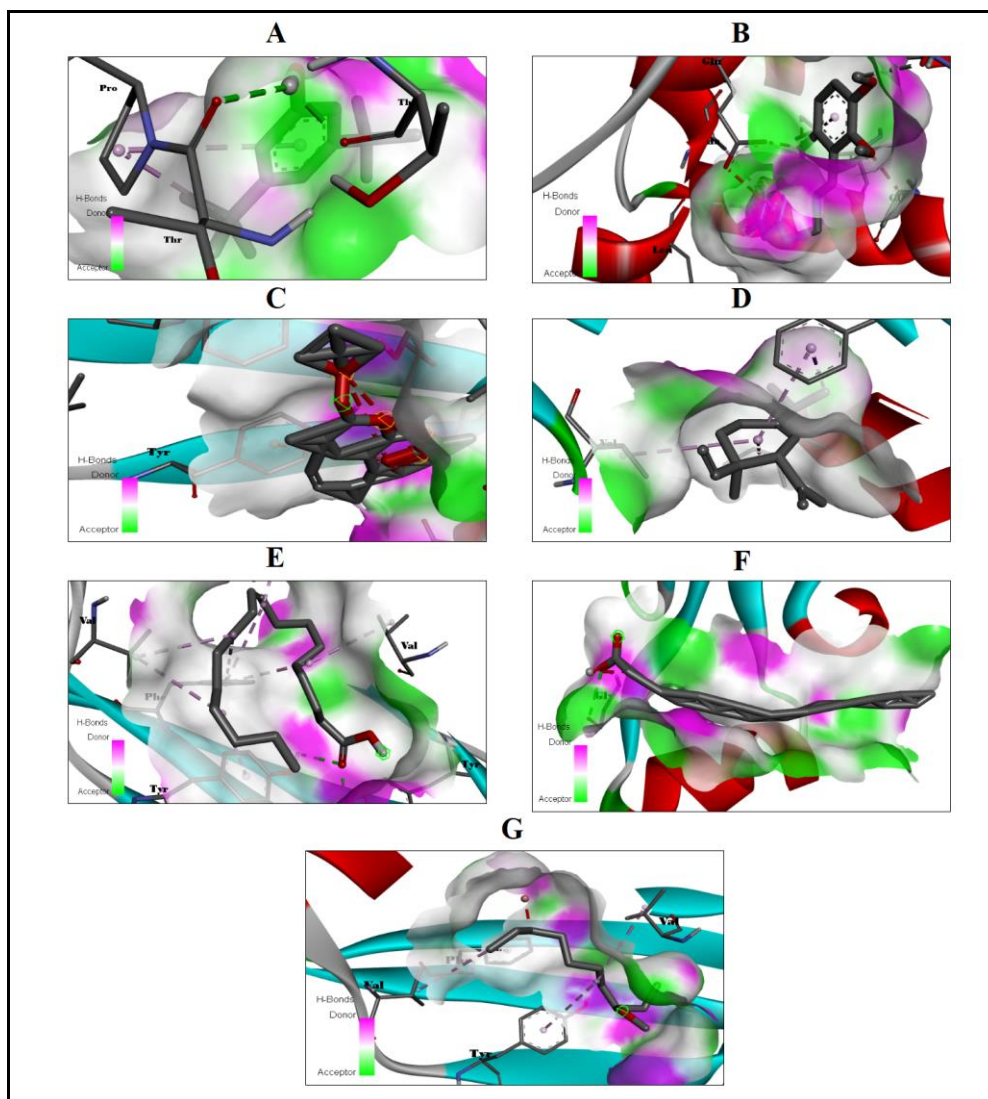


Figure 13. 3D interaction of different ligands with the targeted receptor of *Escherichia coli* FimH protein. (A) Phenol, 3,5-bis(1,1-dimethylethyl), (B) 3-isopropoxy-1,1,1,7,7,7-hexamethyl-3,5,5-tris(trimethylsiloxy)tetrasiloxane, (C) Dihydroartemisinin, 10-o-(t-butylloxy)- (D) Cyclohexanol, 4-ethenyl-4-methyl-3- (E) Oleic acid, (F) Eicosanoic acid, and (G) Ether, 6-bromo-1-ethyloctyl methyl.

645 **Table 6.** Molecular docking scores of selected compounds against and the protein (PDB ID:4XO8 & PDB ID: 1jjj)

Compound	Binding affinity (PDB ID:2jvu)	Binding affinity (PDB ID: 1jjj)	Amino acid interaction	Amino acid interaction
Phenol, 3,5-bis(1,1-dimethylethyl)	-5.49 kcal/mol	-5.93 kcal/mol	THR, PRO and THR	PHE, PHE, and GLU
3-isopropoxy-1,1,1,7,7,7-hexamethyl-3,5,5-tris(trimethylsiloxy)tetrasiloxane	-3.23 kcal/mol	-3.94 kcal/mol	GLU, GLU, LEU, and ALA	SER, GLY, ARG, LYS, and GLU
Dihydroartemisinin, 10-o-(t-butyloxy)-	-9.45 kcal/mol	-9.84 kcal/mol	TYR	LYS, GLY, and ASP
Cyclohexanol, 4-ethenyl-4-methyl-3-(1-methylethenyl)-, [1R-(1 α ,3 α ,4 β)]- [1R-(1 α ,3 α ,4 β)]-	-5.81 kcal/mol	-6.03 kcal/mol	SER, SER, ASP, ALA, PRO, VAL, ASP, TRP, and GLU	LEU
Oleic acid	-3.72 kcal/mol	-5.81 kcal/mol	TYR, VAL, ILE, PHE, and TYR	ILE, LEU, ILE, and LEU
Eicosanoic acid	-1.59 kcal/mol	-1.7 kcal/mol	ALA, PHE, and VAL	GLY, LYS, LEU, PRO, and ILE
Ether, 6-bromo-1-ethyloctyl methyl	-3.96 kcal/mol	-4.04 kcal/mol	PHE, VAL, TYR, and VAL	TRP, HIS, ILE, TYR, ASP, and ILE

646 Note - THR: Threonine, PRO: Proline, GLU: Glutamic acid, LEU: Leucine, ALA: Alanine, TYR: Tyrosine, SER: Serine, ASP: Asparagine, VAL:
647 Valine, TRP: Tryptophan, ILE: Isoleucine, PHE: Phenylalanine, HIS: Histidine, LYS: Lysine, GLY: Glycine, and ARG: Arginine.

648

649 4. DISCUSSION

650 In the current study, the endophytic *A. macrospora* was isolated from the leaves
651 of *T. connaroides* and identified based on fungal morphology, microscopic features, and
652 molecular analysis. In previous reports, the endophytes *Aspergillus* sp., *Cladosporium*
653 sp., *Fusarium* sp., *Phomopsis* sp., *Colletotrichum* sp., *Alternaria* sp., *Diaporthe* sp., and
654 *Trichoderma* sp. were identified based on colony morphology and molecular analysis
655 (Mbilu et al., 2018). Similarly, endophytes *Gliocladium solani* and *Penicillium melinii*
656 from *Artemisia scoparia* with white colonies have been reported (Nisa et al., 2018). In our
657 study, the endophyte *A. macrospora* showed whitish colonies. In the context of this study,
658 the colony morphology of *Alternaria officinalis*, previously isolated by the study group,
659 has been shown to produce wool-like pale gray septal hyphae with linear and curved
660 conidia arranged in linear and bifurcated chains (Ranganathan & Mahalingam, 2019). In
661 this study, *A. macrospora* colonies were grayish green in color and were septal, vitreous,
662 straight, and branched mycelia. In addition, molecular phylogenetic analysis of the 5.8s
663 DNA ITS (500 bp) sequence confirmed that the isolated strain was *A. macrospora*. Using
664 a combined approach of morphological and molecular confirmations, similar reports on
665 the phylogenetic identities and relationships of endophytic fungi isolated from *Artemisia*
666 *indica*, *A. capillaris*, and *A. lactiflora* plant species have been previously documented
667 (Huang et al., 2009).

668 Different groups of endophytic fungi are known to be pioneering producers of
669 bioactive molecules with different configurations and structural arrangements (Schuller et
670 al., 2022). It is a known fact that various organic compounds derived from endophytes
671 have biological activities such as antibacterial, antifungal, antitumor, antioxidant, anti-
672 inflammatory, and larval control (Selvi, 2014). Several endophytes from various medicinal
673 plants have contributed to the fight against emerging infectious diseases including HIV,
674 influenza, malaria, Zika virus, Dengue and foot and mouth disease (Sharma et al., 2016;
675 Kim & Ahn, 2017). These chemicals are produced by *Alternaria* spp. and are effective
676 against insect pest *Spodoptera litura* (Kaur et al., 2019). Some researchers have therefore
677 attempted to link the anti-insect properties of pure or semi-purified extracts or chemicals
678 (Singh et al., 2012; Yang et al., 2012). The study reveals that the ethyl acetate mycelial
679 metabolites of *A. macrospora* exhibit a significant mortality rate of *A. aegypti* larvae
680 (500µg/mL) and showed sensitivity to chemicals present in the mycelial extract. This may
681 support the research to develop new mosquito repellents based on bioactive compounds
682 from fungi on behalf of chemical larvicides (Abutaha et al., 2015). It was found that most

683 endophytes have excellent larval control activity. Thus, *C. ptroselinum* for *Culex pipiens*
684 larvae showed a clear LC₅₀ value of 152.94 µg/mL (Khater & Shalaby, 2008). A novel
685 isoquinoline from *F. moniliforme* against *A. aegypti* and *A. stephensi* showed LC₅₀ of
686 237.0-276.4 ppm (Pradeep et al., 2015). In this study, LC₅₀ and LC₉₀ values were found to
687 be 96.167 to 143.864 µg/mL and 395.16 to 655.77 µg/mL, respectively, for the 1st to 4th
688 instar larvae of *A. aegypti*. The values shown indicate the concentration of the tested
689 substance or treatment needed to kill, in percentage terms (either 50% or 90%), the *A.*
690 *aegypti* larvae at the respective larval instar. The study most likely attempted to determine
691 if a specific medicine or therapy was effective in controlling or becoming eliminate of
692 these mosquito larvae. Similar studies have reported on the mosquito and larval-killing
693 properties of the fungus *A. terreus* against *A. stephensi* (LC₅₀=97.410, 102.551, 29.802,
694 and 8.907; LC₉₀=767.957, 552.546, 535.474, and 195.677 µg/mL) and *A. aegypti*
695 (LC₅₀=83.541, 84.418, 80.407, and 95.926; LC₉₀=515.464, 443.167, 387.910, and 473.998
696 µg/mL). (Ragavendran and Natarajan 2015).

697

698 Vyas et al. (2007) found 100% mortality when the metabolites of the fungus
699 *Lagenidium giganteum* were treated with 1st instar larvae of *A. aegypti*, *C. quinquefasciatus*
700 and *An. stephensi*. In our study, 500 µg/mL *A. macrospora* extract showed 100%
701 mortality in 1st instar larvae. Fungal metabolites or spores can disrupt the cuticle's integrity
702 and pigmentation on the outside while also altering lipid, carbohydrate, and protein
703 metabolism on the inside, impairing insect growth and reproduction, and triggering
704 immunological reactions (Vivekanandhan et al., 2020). Before metabolites attach to
705 phosphorus from DNA or sulfur from proteins and cause denaturation of organelles and
706 enzymes in insects, it is known that fungal metabolites puncture the exoskeleton (Masi et
707 al., 2017) and reach the intracellular region. Reactive oxygen species (ROS) production is
708 one of the most severe cellular consequences brought on by metabolite exposure, and
709 three basic processes have been put out to explain how this happens in living organisms.
710 Metabolites can be internalized into the cell by (1) endocytosis; (2) formation of the
711 endocytotic vesicles; and (3) release of compounds/substances from vesicles into the cell.
712 The primary causes of ROS production by metabolites include the following: parameters
713 involved with the physicochemical characteristics (size, shape, properties, and surface
714 chemistry); interactions with the mitochondria; and the relationship to NADPH oxidase.
715 These components trigger the production of ROS and all of its aftereffects, which include
716 cellular membrane damage, mutations in DNA, cell cycle arrest, and changes in apoptosis

717 (Tunçsoy, 2018). Dharumadurai et al. (2010) have reported 23 isolates of actinomycetes,
718 in which *Streptomyces* sp. showed remarkable activity against *Anopheles* sp. Wherein,
719 the present study the LC₅₀ and LC₉₀ values for mycelial metabolites from *A. macrospora*
720 ranged from 234.390 to 739.362 µg/mL with the impact on pupal development of *A.*
721 *aegypti*. A similar report by Murugan et al. (2011) stated the insecticidal and pupicidal
722 effects of *M. anisopliae* against the malaria mosquito *A. stephensi*. Ragavendran et al.
723 (2017) analyzed the insecticidal and pupicidal effects of the entomopathogenic fungus *B.*
724 *bassiana* against three targeted mosquitoes. The *A. macrospora* extract also showed
725 promising ovicidal activity due to the bioactive metabolites present in the extract. Al-
726 Mekhlafi (2018) has reported on the ovicidal activity and histopathological changes
727 induced by the *Carum copticum* extract against *C. pipiens*. In our study, 100% ovicidal
728 activity was observed in *A. aegypti* and LC₅₀ was 36.08 µg/mL. The rate of hatching was
729 found to be inversely proportional to the concentration of the extract. Reegan et al. (2013)
730 reported an LC₅₀ value of 62.5 ppm of *Clionacelata* extract for eggs of *C. quinquefasciatus*
731 and *A. aegypti*. Martínez et al. (2007) have screened the ethanol extracts of five sponges,
732 *Ircinia campana*, *Amphimedon compressa*, *Agelas sventres*, *Topsentia ophiraphidites*,
733 and *Svenzea zeai*, were screened against larvae and eggs of *C. quinquefasciatus* and *A.*
734 *aegypti*.

735 The increase in resistance is a crucial concern because arthropod-borne diseases
736 are addressed mainly by insecticide-based vector activity (Gan et al., 2021). Southeast Asia
737 is noticing an increase in insecticide resistance, continuing the worldwide trend of other
738 types of resistance (WHO, 2023). Natural ingredients may be used as potential
739 insecticides to manage disease vectors due to their accessibility and safety, which would
740 minimize the number of synthetic pesticides (Lengai et al., 2020). Insects exposed to
741 fungal-based biopesticides may experience upregulation or downregulation in their whole-
742 body protein levels (Li et al., 2019; Parthiban et al., 2021). The findings strengthen the
743 probability that *A. aegypti* mortality may be connected to the inhibition of enzyme activity
744 by *A. macrospora*.

745 Our research found that the AChE activity of the 4th instar larvae exposed to
746 fungus metabolites were significantly lower than those of the control larvae. Similarly,
747 Ragavendran et al. (2019) observed that treatment with *Penicillium* sp. metabolites
748 decreased the AChE activity in *A. aegypti* and *C. quinquefasciatus* larvae. AChE is a
749 neurotransmitter molecule that hydrolyses acetylcholine into acetate and choline
750 (Rajagopalan et al., 2023). Pre-synaptic neurons constantly release acetylcholine into the

751 synaptic cleft, interacting with receptor/ligand-gated sodium channels, enabling the
752 sodium ions to transport rapidly through this channel (Oni et al., 2019). One of the
753 fundamental resistance mechanisms in insect pests, AChE change, has been identified to
754 be resistant to carbamate and organophosphorus (Ghosh et al., 2012). Fungal active
755 molecules may bind to and decrease the activity of the enzyme AChE, which destroys
756 acetylcholine, a key neurotransmitter in the central nervous system of insects (Rants'o et
757 al., 2022). AChE inhibitory properties of fungal metabolites have been reported (Zibae
758 et al., 2009; Abraham et al., 2015; Santra et al., 2022). The result that larvae died after
759 being exposed to fungus mycelial metabolites demonstrated that the chemical in the
760 metabolites might interfere with the cholinergic connection and interrupt the network of
761 exonic communication, inhibiting the release of nerve signals. Thus, the lethal effect may
762 result from a build-up of the neurotransmitter acetylcholine at synaptic junctions,
763 disrupting coordination between the nerve and muscle connections (Jankowska et al.,
764 2018). According to an earlier finding, AChE inhibitors slow larvae growth, reduce the
765 hatching of treated eggs, and negatively impact insect behavior (Al-Massarani et al., 2019).

766 To the best of our knowledge, this is the first data available for the
767 histopathological study of *A. macrospora* mycelial metabolites against targeted
768 mosquitoes. The present work has demonstrated that tested mycelial metabolites led to
769 histological changes in the midgut component of *A. aegypti* larvae, including food bolus,
770 epithelial cells, microvilli, and gastric caeca. In the midgut, there were irregular shapes for
771 the epithelial cells, microvilli, and Epithelium and breaks in the food bolus and
772 peritrophic membrane. According to a recent study, 4th instar *A. stephensi*, *A. aegypti* and
773 *C. pipiens* larvae treated with the entomopathogenic fungus *Metarhizium*
774 *anisopliae* displayed numerous histological alterations and malformations in body tissues.
775 They affected various body parts, particularly the cuticle, adipose cells, and midgut
776 region, compared to untreated larvae (Vivekanandhan et al., 2022). Likewise, Abutaha et
777 al. (2015) observed that *Aspergillus sydowi* metabolites were administered against *A.*
778 *caspius* caused disintegration of the peritrophic membrane, cytoplasmic vacuolization,
779 and malformations of cellular microvilli in the larvae pathological pattern.

780 Many secondary metabolites produced by plant endophytic and pathogenic fungi
781 are significant for toxicity and interaction with other pathogens (Narayanan & Glick,
782 2022). Some of these natural products can display strong biocidal activity against human
783 pathogenic microorganisms due to their broad-spectrum action (Jakubczyk & Dussart,
784 2020). The discovery and production of medicines for treating human diseases depend

785 heavily on natural products, and the microbial environment is a significant source of new
786 bioactive substances (Cruz et al., 2020). The pharmacological diversity of *Alternaria*
787 fungus, such as the production of phytotoxins and mycotoxins, is also well documented
788 (Lou et al., 2013; Tsuge et al., 2013). Over the past few decades, at least 268
789 biomolecules with phytotoxic, cytotoxic, and antibacterial activities have been discovered
790 in *Alternaria* fungus (Brase et al., 2009; Dalinova et al., 2020; Al Mousa et al., 2021). The
791 antibacterial activity of mycelial extracts has been reported in many studies (Sharma et al.,
792 2016). Santos et al. (2015) have reported the endophytes from the leaves of *I. suffruticosa*
793 against bacterial pathogens such as *B. subtilis* and *E. coli*. In our study, it was found that
794 *A. macrospora* mycelium metabolites strongly inhibit *E. coli* (22 mm), *B. subtilis* (19
795 mm), *S. aureus* (20 mm), and *S. typhi* (16 mm). Thus, in this study, the fungal metabolites
796 may be caused by bacteriostatic action on the test bacteria by disrupting their cell
797 membranes. The test bacteria were inhibited as the outcome of the respiratory chain of
798 the bacteria being inactivated, which also affected the oxidative phosphorylation and
799 tempered the generation of energy route of the bacteria (Maliehe et al., 2022). Thus, it
800 may be stated that the extract suppressed the test bacterium by obstructing the respiratory
801 chain dehydrogenase function. The findings are consistent with the research of Gooma,
802 (2017), which found that antimicrobial drugs might work by interfering with the function
803 of bacterial respiratory cycle dehydrogenase.

804
805

806 These outcomes agree with the findings of Maliehe et al. (2022), which showed
807 that the ethyl acetate extract inhibited *S. aureus* and *E. coli* by puncturing their cell
808 membranes. Makut and Owolewa (2011) reported the inhibitory activity of the
809 endophytes *A. flavus* and *A. niger* against *S. aureus* and *E. coli*. Petit et al. (2009) have
810 studied the activities of *Penicillium* sp. against *Streptococcus pyogenes*, *S. typhimurium*,
811 and *B. cereus*. Premjanu et al. (2016) have noticed the largest inhibitory zone against
812 *Malassezia pachydermis* from *A. niger*. In a crude extract of *Alternaria* sp., the compound
813 oleic acid was detected with antifungal properties against phytopathogenic species of
814 *Moniliophthora perniciosa* and *P. ultimum* (Walters et al., 2004). In agreement with the
815 earlier findings, the oleic acid compound in the mycelial extract of *A. macrospora*
816 exhibited excellent antibacterial activity against clinical pathogens such as *E. coli* and *S.*
817 *aureus* (Zhang et al., 2023).

818 The present study also showed that the cytotoxic activity of mycelium metabolites
819 against HeLa cells was tested by MTT assay. The fungal metabolites showed 68%
820 cytotoxicity at 300 µg/mL concentration and were significantly active against cancer cells
821 (IC₅₀ value 118.49 µg/mL). Likewise, Kumari et al. (2018) have reported the cytotoxic
822 activity of the endophyte *Talaromyces purpureogenus* against HeLa and MCF7 cell lines.
823 Itsuki et al. (2007) reported that the cytotoxic effect was exhibited in several phenolic
824 metabolites from *Alternaria* L5178Y mouse lymphoma cells. Similarly, Artika et al.
825 (2017) have reported the anticancer activity of the endophyte *Phomopsis* sp. against an
826 MCF7 cell line with an IC₅₀ of 19.2 µg/mL. Huang et al. (2012) reported that the
827 Alterporriol L, a bianthraquinone derivative found in the marine fungus *Alternaria* sp.
828 ZJ9-6B inhibited the MDA-MB-435 breast cancer cells from proliferating and growing by
829 damaging their mitochondria. Earlier, Ragavendran and Natarajan (2015) investigated the
830 mycelial metabolites of *A. terreus* and its components, showing that the chemical (phenol,
831 3,5-bis(1,1-dimethylethyl) had more potent insecticidal and pupicidal effects on *C.*
832 *quinquefasciatus*, *An. stephensi* and *A. aegypti*. In support, the presently revealed
833 compound phenol, 3,5-bis(1,1-dimethylethyl) (4.57%) from the *A. macrospora* might exert
834 antifungal activity. Likely, Sharma et al. (2016) have evaluated the bioactive secondary
835 metabolites isolated from the endophyte *Pestalotiopsis neglecta* contained oleic acid as
836 similar to the GC-MS of *A. macrospora* metabolite, i.e., oleic acid (22.093%) with a
837 higher peak than other compounds. The GC-MS analysis of *A. macrospora* metabolites
838 results clearly show that seven major chemical constituents namely phenol, 3,5-bis(1,1-
839 dimethylethyl), 3-isopropoxy-1,1,1,7,7,7-hexamethyl-3,5,5-
840 tris(trimethylsiloxy)tetrasiloxane, ether, 6-bromo-1-ethyloctyl methyl, dihydroartemisinin,
841 10-o-(t-butyloxy)-, oleic acid and eicosanoic acid. Among the chemical constituents, oleic
842 acid and eicosanoic acid as major chemical ingredients found in the fungal metabolites, so
843 these chemical constituents may be involved in mosquito larvicidal activity. Earlier
844 research found that, *B. bassiana*, *A. tamarii*, and *A. terreus* secondary
845 metabolites/essential oils contain similar kinds of organic chemical constituents with
846 larvicidal and pupicidal activities against targeted mosquitoes (Ragavendran and Natarajan,
847 2015; Ragavendran et al., 2017; Baskar et al., 2020). The GC-MS analysis of the
848 endophyte *Curvularia aeria* contained eicosene (7.93%), which is quite similar to the peak
849 area (9.047%) of the presently revealed eicosanoic acid from *A. macrospora* (Sahani and
850 Thakur, 2019). FT-IR is commonly used to identify chemical constituents' functional
851 groups and helps elucidate compounds (Starlin et al. 2012). Our FT-IR results showed

852 the presence of phenolic compounds, alkenes, and amines based on wavenumber, peak
853 assignment, and vibration mode. Similarly, CH stretches of alkene groups in ethyl acetate
854 extracts of the endophytes *Chaetomium globosum*, *Penicillium janthinellum*, and
855 *Cladosporium tenuissimum* were reported from an earlier study at 2855.08 cm⁻¹ (Kanjana
856 et al. 2019). The mycelium extract of *A. macrospora* also confirmed the corresponding
857 alcohols, carboxylic acids, alkene, and other minor proportions. These functional groups
858 may be involved in mosquito larvicidal, cytotoxicity, and antibacterial activity. Similarly,
859 Ragavendran et al. (2019) and Vivekanandhan et al. (2018) stated that the *Penicillium* sp.
860 and *B. bassiana*-28 derived metabolites have similar functional groups, respectively.
861 Furthermore, the main peaks of 3317.54 and 2924.09 cm⁻¹ were assigned to the functional
862 groups of alkyl (= CH stretch), which resemble intense peaks (3300.20 and 2924.09 cm⁻¹)
863 representing aromatic and alkene-based CH stretches from the crude extract of *C.*
864 *gloeosporioides* (Rabha et al. 2015). However, more studies on identifying active
865 compounds and semi-field trials are necessary before suggesting the active ingredients of
866 microbial metabolites for establishing eco-friendly mosquito vector control strategies.

867 Zebrafish models are used for drug screening and toxicity analysis due to their
868 genetic similarity, short life cycle, and cost-effectiveness. Using zebrafish embryos/larvae,
869 the toxicity range of the bioactive compounds or plant extract can be predicted (Siddhu et
870 al., 2022). To use microbial metabolites as eco-friendly mosquito vectors, their extract
871 toxicity range was tested in the zebrafish model. The toxic exposure to the zebrafish
872 larvae causes the development of malformation. In the meantime, the increased extract
873 concentration affects the survival, heart rate, and hatching rate of the embryos/larvae as
874 well as causes BT and YSE development in the larvae. Likewise, Cao et al. (2016)
875 detected physiological and morphological changes in zebrafish treated with cyhalofop-
876 butyl, as well as a decreased rate of embryonic development, delayed autonomous
877 movement, a decreased pulse, and embryos with shortened body lengths (at higher
878 doses). Similarly, Abutaha et al. (2015) reported that *Cochliobolus spicifer* endophytic
879 fungal extract produces minor anomalies or deformities in zebrafish embryos. The latest
880 report by Taher et al. (2022) on endophytic *Phyllosticta fallopiae* molecules found
881 teratogenic and low toxicity in zebrafish models, with a concentration-dependent
882 correlation.

883 Further, the *in-silico* toxicity analysis was performed for each microbial metabolite
884 to identify its toxic nature. All the metabolites showed a non-toxic condition except oleic
885 acid. Even oleic acid was less harmful, which may be why they have not demonstrated

886 toxic effects in zebrafish developmental toxicity analysis. The *in-silico* and *in-vivo* toxicity
887 analysis confirmed that these metabolites are not toxic and can be used as eco-friendly
888 vectors. The mycelium extract was tested for antimicrobial activity, and they showed
889 better results. But their specific mechanisms of interaction with pathogen receptors are
890 not known. So that through the molecular docking analysis, metabolites binding affinity
891 towards the target of *E. coli* FimH protein and *S. aureus* tyrosyl-RNA synthetase protein
892 was performed. Bacteria translocation to the intestinal epithelium causes the life-
893 threatening disease of sepsis (Sun et al., 2022). FimH helps the *E. coli* with translocation
894 so that compound that interacts and acts as an inhibitor helps prevent the infection (Poole
895 et al., 2017). *S. aureus* tyrosyl-RNA synthetase protein is mainly involved in converting the
896 covalently amino acid to tRNA (Elkolli et al., 2023). The compound that specifically binds
897 to this receptor helps inhibit the protein synthesis process (Athar et al., 2020). In our
898 findings, all the metabolites showed good binding affinity and amino interaction toward
899 the target protein. Among the metabolites, dihydroartemisinin, 10-o-(t-butylloxy)- led the
900 better binding affinity in both the targeted receptor. This could be the reason for the
901 effective antibacterial activity of mycelium extract against the tested pathogens.

902

903 5. CONCLUSION

904 Overall, this study shed light on the endophytic fungus *A. macrospora* isolated
905 from the medicinal plant *T. connaroides* based on conventional morphological (colony
906 morphology and conidia structure) and molecular (ITS region amplification) approaches.
907 In conclusion, *A. macrospora* fungal metabolite produced 100% mortality in larvae of *A.*
908 *aegypti*, after 24 h exposure. They were followed by the 100% of mortality of pupae
909 observed at the concentration of mycelium metabolite (500 µg/mL). Hatchability is
910 significantly inhibited at 500 µg/mL of the metabolites of *A. macrospora*. Fungus
911 metabolites significantly reduced AChE enzyme activity in the larvae. The control
912 group histological study confirmed that the midgut epithelium is made up of a single layer
913 of digesting cells with well-developed cytoplasmic and brush borders. Severe damage to
914 the treated group included the hindgut, vacuolated cells, particularly damaged epithelium
915 larvae, collapse of the epithelial barrier and exterior cuticle, and internal membranes. In
916 addition, four different pathogens were used to evaluate the antibacterial properties of
917 four different mycelia metabolite concentrations (25, 50, 75, and 100 µg/mL). *E. coli*
918 exhibited the broadest zone of growth inhibition (22 mm), followed by *S. aureus* (20
919 mm), *B. subtilis* (19 mm), and *S. typhi* (14 mm). Furthermore, the fungal constituents

920 resulted in the IC₅₀ value of 118 µg/mL on HeLa cells using MTT assay, indicating that the
921 metabolites are cytotoxic. GC-MS analysis showed the presence of potential secondary
922 metabolites, namely cyclohexanol, 4-ethenyl-4-methyl-3-(1-methylethenyl) (15.284%),
923 eicosanoic acid (9.047%), ether, 6-bromo-1 ethyloctyl methyl (4.182%) and oleic acid
924 (22.093%). Further, the functional groups were identified from the *A. macrospora* using
925 the FT-IR spectrum. Meanwhile, the *in-silico* and *in-vivo* zebrafish larvae toxicity
926 prediction confirmed that they are non-toxic. Finally, the metabolite's antibacterial
927 potential was confirmed by interacting with specific *E. coli* and *S. aureus* receptors. The
928 results clearly indicate that these metabolites can be used as antimicrobial agents with
929 lesser toxic effects.

930

931 6. ACKNOWLEDGEMENTS

932 The authors thanked the Periyar University administration for providing the
933 laboratory space needed to conduct this research. The DST-FIST [SR/FIST/LSIS-
934 673/2016], a substantial award to the Biotechnology Department, is gratefully
935 acknowledged by the authors of Periyar University for their assistance in boosting the
936 instrumentation infrastructure. Furthermore, the authors thank the National Council for
937 Scientific and Technological Development for the financial support. Malafaia G. holds a
938 productivity scholarship from CNPq (Proc. #308854/2021-7). Liverpool John Moores
939 University supported the work.

940

941 7. AUTHOR CONTRIBUTIONS

942 **CR and CK:** planned the research, conducted the experiments, shared chemicals,
943 analyzed the tools, and wrote the manuscript. **CR and DN:** conceptualization,
944 methodology, and performed the embryotoxicity experiments. **CR, GM, and CK:** writing,
945 reviewing, and editing. **IN, TC, VM, MK, and GM** revised the manuscript All authors
946 have read and decided on the published version of the manuscript.

947

948 8. DECLARATION OF COMPETING INTEREST

949 We validated that there were no known conflicts of interest related to this work,
950 and there was no significant financial backing that might have affected how it turned out.
951 We also guarantee that all identified writers have read, reviewed, and authorized the
952 manuscript and that no other individuals who meet the requirements for authorship but

953 are not mentioned have contributed. The integrity of the work has been guaranteed with
954 proper attention.

955

956 **9. ETHICAL ASPECTS**

957 All experimental methods were carried out in accordance with the ethical
958 guidelines for using animals in research, and special care was taken to minimize the
959 animals' suffering and external causes of tension, pain, and discomfort. The quantity of
960 animals used in the present study is within the range required to generate valid scientific
961 data. No research involving human subjects was referenced in this paper by any authors.

962

963 **10. AVAILABILITY OF DATA AND MATERIALS**

964 The datasets used and/or analyzed during the current study are available from the
965 corresponding author upon reasonable request.

966

967 **11. CONSENT TO PARTICIPATE**

968 Not applicable.

969

970 **12. CONSENT TO PUBLISH**

971 Not applicable.

972

973 **13. REFERENCES**

974

975 Abbott, W. S. 1925. A method of computing the effectiveness of an insecticide. *J. Econ.*

976 *Entomol.* 18: 265-266

977 Abdelaziz, R., Tartor, Y. H., Barakat, A. B., El-Didamony, G., Gado, M. M., &

978 Berbecea, A. (2023). Bioactive metabolites of *Streptomyces misakiensis* display

979 broad-spectrum antimicrobial activity against multidrug-resistant bacteria and

980 fungi. *Frontiers in Cellular and Infection Microbiology*, 13, 1162721.

981 Abraham, S., Basukriadi, A., Pawiroharsono, S., & Sjamsuridzal, W. (2015). Insecticidal

982 activity of ethyl acetate extracts from culture filtrates of mangrove fungal

983 endophytes. *Mycobiology*, 43(2), 137-149.

984 Abutaha, N., Mashaly, A. M., Al-Mekhlafi, F. A., Farooq, M., Al-shami, M., & Wadaan,

985 M. A. (2015). Larvicidal activity of endophytic fungal extract of *Cochliobolus*

986 *spicifer* (Pleosporales: Pleosporaceae) on *Aedes caspius* and *Culex pipiens*
987 (Diptera: Culicidae). *Applied entomology and zoology*, 50, 405-414.

988 Al Mousa, A. A., Mohamed, H., Hassane, A. M., & Abo-Dahab, N. F. (2021).
989 Antimicrobial and cytotoxic potential of an endophytic fungus *Alternaria*
990 *tenuissima* AUMC14342 isolated from *Artemisia judaica* L. growing in Saudi
991 Arabia. *Journal of King Saud University-Science*, 33(5), 101462.

992 Al-Massarani, S., El-Shaibany, A., Tabanca, N., Ali, A., Estep, A. S., Becnel, J. J., ... &
993 Baser, K. H. C. (2019). Assessment of selected Saudi and Yemeni plants for
994 mosquitocidal activities against the yellow fever mosquito *Aedes aegypti*. *Saudi*
995 *Pharmaceutical Journal*, 27(7), 930-938.

996 Al-Qaralleh, O. S., Al-Zereini, W. A., & Al-Mustafa, A. H. (2021). Antibacterial,
997 antioxidant and neuroprotective activities of crude extract from the endophytic
998 fungus *Fusarium* sp. isolate OQ-Fus-2-F from *Euphorbia* sp. plant. *Journal of*
999 *Pharmacy & Pharmacognosy Research*, 9(6), 755-765.

1000 Álvarez Valverde, V., Rodríguez Rodríguez, G., & Argüello Vargas, S. (2022). Bioguided
1001 Phytochemical Study of *Ipomoea cairica* Extracts with Larvicidal Activity against
1002 *Aedes aegypti*. *Molecules*, 27(4), 1348.

1003 Araújo, I. F., Marinho, V. H. D. S., Sena, I. D. S., Curti, J. M., Ramos, R. D. S.,
1004 Ferreira, R., ... & Ferreira, I. M. (2022). Larvicidal activity against *Aedes aegypti*
1005 and molecular docking studies of compounds extracted from the endophytic
1006 fungus *Aspergillus* sp. isolated from *Bertholletia excelsa* Humn. &
1007 Bonpl. *Biotechnology Letters*, 44(3), 439-459.

1008 Ashutosh, S., & Pati, P. K. (2011). First record of 28-spotted ladybird beetle,
1009 *Henosepilachna vigintioctopunctata* (F.) infesting *Withania somnifera* (L.) dunal
1010 in Punjab Province of Northern India. *Pest Technology*, 5(1), 91-92.

1011 Bacha, K., Tariku, Y., Gebreyesus, F., Zerihun, S., Mohammed, A., Weiland-Bräuer,
1012 N., ... & Mulat, M. (2016). Antimicrobial and anti-Quorum Sensing activities of
1013 selected medicinal plants of Ethiopia: Implication for development of potent
1014 antimicrobial agents. *BMC microbiology*, 16, 1-9.

1015 Baskar, K., Chinmasamy, R., Pandey, K., Venkatesan, M., Sebastian, P. J., Subban, M., ...
1016 & Devarajan, N. (2020). Larvicidal and histopathology effect of endophytic
1017 fungal extracts of *Aspergillus tamarii* against *Aedes aegypti* and *Culex*
1018 *quinquefasciatus*. *Heliyon*, 6(10), e05331.

- 1019 Beltrán, M., & Lozano, L. C. (2022). Synergistic larvicidal activity of *Metarhizium*
1020 *anisopliae* and *Azadirachta indica* extract against the malaria vector *Anopheles*
1021 *albimanus*. *International Journal of Tropical Insect Science*, 1-8.
- 1022 Bhadra, F., Gupta, A., Vasundhara, M., & Reddy, M. S. (2022). Endophytic fungi: a
1023 potential source of industrial enzyme producers. *3 Biotech*, 12(4), 86.
- 1024 Bräse, S., Encinas, A., Keck, J., & Nising, C. F. (2009). Chemistry and biology of
1025 mycotoxins and related fungal metabolites. *Chemical reviews*, 109(9), 3903-
1026 3990.
- 1027 Brase, S., Encinas, A., Keck, J., & Nising, C. F. (2009). Chemistry and biology of
1028 mycotoxins and related fungal metabolites. *Chemical reviews*, 109(9), 3903-3990
- 1029 Cao, F., Liu, X., Wang, C., Zheng, M., Li, X., Qiu, L., 2016. Acute and short-term
1030 developmental toxicity of cyhalofop-butyl to zebrafish (*Danio rerio*). *Environ Sci*
1031 *Pollut Res.* 23(10), 10080-10089.
- 1032 Cara, M., Toska, M., Frasherri, D., Baroncelli, R., & Sanzani, S. M. (2022). *Alternaria*
1033 species causing pomegranate and citrus fruit rots in Albania. *Journal of Plant*
1034 *Diseases and Protection*, 129(5), 1095-1104.
- 1035 Cazal, C. M., Matos, A. P., Domingues, V. D. C., Cunha, G. O. S., Vieira, P. C., da
1036 Silva, M. F. D. G. F., & Fernandes, J. B. (2023). Limonoids and insecticidal activity
1037 on *Spodoptera frugiperda* (JE Smith)(Lepidoptera: Noctuidae) of *Trichilia catigua*
1038 A. Juss.(Meliaceae). *Zeitschrift für Naturforschung C*, 78(5-6), 229-233.
- 1039 Chatterjee, S., Bag, S., Biswal, D., Paria, D. S., Bandyopadhyay, R., Sarkar, B., ... &
1040 Dangar, T. K. (2023). Neem-based products as potential eco-friendly mosquito
1041 control agents over conventional eco-toxic chemical pesticides-A review. *Acta*
1042 *Tropica*, 106858.
- 1043 Chauhan, A. S., Prinja, S., Srinivasan, R., Rai, B., Malliga, J. S., Jyani, G., ... & Ghoshal,
1044 S. (2020). Cost effectiveness of strategies for cervical cancer prevention in
1045 India. *PLoS One*, 15(9), e0238291.
- 1046 Cruz, J. S., da Silva, C. A., & Hamerski, L. (2020). Natural products from endophytic
1047 fungi associated with Rubiaceae species. *Journal of Fungi*, 6(3), 128.
- 1048 da Silva Sa, G. C., Bezerra, P. V. V., da Silva, M. F. A., da Silva, L. B., Barra, P. B., de
1049 Fátima Freire de Melo Ximenes, M., & Uchoa, A. F. (2023). Arbovirus vectors
1050 insects: are botanical insecticides an alternative for its management?. *Journal of Pest*
1051 *Science*, 96(1), 1-20.

1052 da Silva, O.S., Prado, G.R., da Silva, J.L.R. *et al.* Oral toxicity of *Photorhabdus*
1053 *luminescens* and *Xenorhabdus nematophila* (Enterobacteriaceae) against *Aedes*
1054 *aegypti* (Diptera: Culicidae). *Parasitol Res* **112**, 2891-2896 (2013).
1055 <https://doi.org/10.1007/s00436-013-3460-x>

1056 Dahran, N., Abd-Elhakim, Y. M., Mohamed, A. A. R., Abd-Elsalam, M. M., Said, E.
1057 N., Metwally, M. M., ... & El-Shetry, E. S. (2023). Palliative effect of *Moringa*
1058 *olifera*-mediated zinc oxide nanoparticles against acrylamide-induced
1059 neurotoxicity in rats. *Food and Chemical Toxicology*, *171*, 113537.

1060 Dalinova, A., Chisty, L., Kochura, D., Garnyuk, V., Petrova, M., Prokofieva, D., ... &
1061 Berestetskiy, A. (2020). Isolation and bioactivity of secondary metabolites from
1062 solid culture of the fungus, *Alternaria sonchi*. *Biomolecules*, *10*(1), 81.

1063 de la Torre-Anzures, J., Figueroa-Brito, R., Carrasco-Aquino, R. J., Garcia-Serrano, L.
1064 A., Ramos-Lopez, M. A., Sotelo-Leyva, C., ... & Lopez-Olguin, J. F. (2023).
1065 Chemical Compounds of Ethanolic Extract from *Trichilia havanensis* Seeds and
1066 its Insecticidal Activity. *Chemistry of Natural Compounds*, 1-4.

1067 de Souza Passos, M., Monteiro, N., Kanashiro, M. M., Braz-Filho, R., & Vieira, I. J. C.
1068 (2022). New hydroperoxycycloartane—complete chemical shifts assignment of
1069 ¹³C and ¹H—and cytotoxicity evaluation of cycloartanes isolated from *Trichilia*
1070 *casaretti*. *Natural Product Research*, *36*(21), 5423-5428.

1071 EFSA Panel on Contaminants in the Food Chain (CONTAM). (2011). Scientific
1072 opinion on the risks for animal and public health related to the presence of
1073 *Alternaria* toxins in feed and food. *EFSA journal*, *9*(10), 2407.

1074 Elawady, M. E., Hamed, A. A., Alsallami, W. M., Gabr, E. Z., Abdel-Monem, M. O.,
1075 & Hassan, M. G. (2023). Bioactive Metabolite from Endophytic *Aspergillus*
1076 *versicolor* SB5 with Anti-Acetylcholinesterase, Anti-Inflammatory and Antioxidant
1077 Activities: In Vitro and In Silico Studies. *Microorganisms*, *11*(4), 1062.

1078 Elghaffar, R. Y. A., Amin, B. H., Hashem, A. H., & Sehim, A. E. (2022). Promising
1079 endophytic *Alternaria alternata* from leaves of *Ziziphus spina-christi*: phytochemical
1080 analyses, antimicrobial and antioxidant activities. *Applied Biochemistry and*
1081 *Biotechnology*, *194*(9), 3984-4001.

1082 Elkolli, M., Elkolli, H., Alam, M., & Benguerba, Y. (2023). In silico study of
1083 antibacterial tyrosyl-tRNA synthetase and toxicity of main phytoconstituents from
1084 three active essential oils. *Journal of Biomolecular Structure and Dynamics*, 1-13.

1085 Ferreira, Q. R., Lemos, F. F. B., Moura, M. N., Nascimento, J. O. D. S., Novaes, A. F.,
1086 Barcelos, I. S., ... & Melo, F. F. D. (2023). Role of the Microbiome in *Aedes* spp.
1087 Vector Competence: What Do We Know?. *Viruses*, *15*(3), 779.

1088 Finney, D. J. 1971. Probit analysis-a statistical treatment of the sigmoid response curve,
1089 3rd ed., p.333. Cambridge University Press, London

1090 Freitas, Í. N., Dourado, A. V., da Costa Araújo, A. P., de Souza, S. S., da Luz, T. M.,
1091 Guimarães, A. T. B., ... & Malafaia, G. (2023). Toxicity assessment of SARS-CoV-
1092 2-derived peptides in combination with a mix of pollutants on zebrafish adults: a
1093 perspective study of behavioral, biometric, mutagenic, and biochemical
1094 toxicity. *Science of The Total Environment*, *858*, 159838.

1095 G.L. Ellman, K.D. Courtney, V. Andres Jr., R.M. Featherstone, A new and rapid
1096 colorimetric determination of acetylcholinesterase activity,, *Biochem.*
1097 *Pharmacol.* 7 (1961) 88-95.

1098 Gan, S. J., Leong, Y. Q., bin Barhanuddin, M. F. H., Wong, S. T., Wong, S. F., Mak, J.
1099 W., & Ahmad, R. B. (2021). Dengue fever and insecticide resistance in *Aedes*
1100 mosquitoes in Southeast Asia: a review. *Parasites & vectors*, *14*(1), 1-19.

1101 Ganesan, P., Samuel, R., Mutheeswaran, S., Pandikumar, P., Reegan, A. D., Aremu, A.
1102 O., & Ignacimuthu, S. (2023). Phytochemicals for mosquito larvicidal activity
1103 and their modes of action: A review. *South African Journal of Botany*, *152*, 19-
1104 49.

1105 Ghosh, A., Chowdhury, N., & Chandra, G. (2012). Plant extracts as potential mosquito
1106 larvicides. *The Indian journal of medical research*, *135*(5), 581.

1107 Gomaa, E. Z. (2017). Silver nanoparticles as an antimicrobial agent: A case study on
1108 *Staphylococcus aureus* and *Escherichia coli* as models for Gram-positive and Gram-
1109 negative bacteria. *The Journal of general and applied microbiology*, *63*(1), 36-43.

1110 Guilherme Malafaia , Andreza Martins de Souza , Aryelle
1111 Canedo Pereira , Stênio Gonçalves , Amanda Pereira da Costa Araújo , Renan
1112 Xavier Ribeiro , Thiago Lopes Rocha. (2020). Developmental toxicity in zebrafish
1113 exposed to polyethylene microplastics under static and semi-static aquatic systems.
1114 *Science of The Total Environment*. Volume 700, 134867.
1115 <https://doi.org/10.1016/j.scitotenv.2019.134867>

1116 Guo, L., Xu, L., Zheng, W. H., & Hyde, K. D. (2004). Genetic variation of *Alternaria*
1117 *alternata*, an endophytic fungus isolated from *Pinus tabulaeformis* as determined by
1118 random amplified microsatellites (RAMS). *Fungal Diversity*.

- 1119 Gupta, M., & Gupta, D. (2022). Essential oils: As Potential Larvicides. *Journal of Drug*
1120 *Delivery and Therapeutics*, 12(3), 193-201.
- 1121 Hazalin, N.A, Ramasamy, K, Lim, S.M, Wahab I.A, Cole, A.L, Majeed, A.B.A. (2009).
1122 Cytotoxic and antibacterial activities of endophytic fungi isolated from plants at the
1123 National Park, Pahang, Malaysia. *BMC Comp Alternative Med.*; 9:46.
1124 <https://doi.org/10.1186/1472-6882-9-46>.
- 1125 He JH, Gao JM, Huang CJ, Li CQ (2014) Zebrafish models for assessing
1126 developmental and reproductive toxicity. *Neurotoxicol Teratol* 42: 35-42
- 1127 Huang, C., Jin, H., Song, B., Zhu, X., Zhao, H., Cai, J., ... & Lin, Y. (2012). The
1128 cytotoxicity and anticancer mechanisms of alterporriol L, a marine
1129 bianthraquinone, against MCF-7 human breast cancer cells. *Applied*
1130 *microbiology and biotechnology*, 93, 777-785.
- 1131 Ismaiel, A. A., Ahmed, A. S., Hassan, I. A., El-Sayed, E. S. R., & Karam El-Din, A. Z.
1132 A. (2017). Production of paclitaxel with anticancer activity by two local fungal
1133 endophytes, *Aspergillus fumigatus* and *Alternaria tenuissima*. *Applied*
1134 *microbiology and biotechnology*, 101(14), 5831-5846.
- 1135 Itsuki Watanabe, Makoto Kakishima, Yoshikazu Adachi, Hiromi Nakajima (2007).
1136 Potential mycotoxin productivity of *Alternaria alternata* isolated from garden
1137 trees. 57 ,1, 3-9
- 1138 Jakubczyk, D., & Dussart, F. (2020). Selected fungal natural products with antimicrobial
1139 properties. *Molecules*, 25(4), 911.
- 1140 Jankowska, M., Rogalska, J., Wyszowska, J., & Stankiewicz, M. (2017). Molecular
1141 targets for components of essential oils in the insect nervous system—A
1142 review. *Molecules*, 23(1), 34.
- 1143 John, R., Sabu, K. R., & Manilal, A. (2022). Chemical Composition, Antioxidant, and
1144 Mosquito Larvicidal Activity of Essential Oils from *Hyptis capitata* Jacq. *Journal*
1145 *of Experimental Pharmacology*, 195-204.
- 1146 Joshi, C. G., Danagoudar, A., Poyya, J., Kudva, A. K., & Dhananjaya, B. L. (2017).
1147 Biogenic synthesis of gold nanoparticles by marine endophytic fungus-
1148 *Cladosporium cladosporioides* isolated from seaweed and evaluation of their
1149 antioxidant and antimicrobial properties. *Process Biochemistry*, 63, 137-144.
- 1150 Jouda, J. B., Mbazona, C. D., Sarkar, P., Bag, P. K., & Wandji, J. (2016). Anticancer and
1151 antibacterial secondary metabolites from the endophytic fungus *Penicillium* sp.

1152 CAM64 against multi-drug resistant Gram-negative bacteria. *African health*
1153 *sciences*, 16(3), 734-743.

1154 Kalimuthu, A. K., Parasuraman, P., Sivakumar, P., Murugesan, S., Arumachalam, S.,
1155 Pandian, S. R. K., ... & Kunjiappan, S. (2022). In silico, in vitro screening of
1156 antioxidant and anticancer potentials of bioactive secondary metabolites from an
1157 endophytic fungus (*Curvularia* sp.) from *Phyllanthus niruri* L. *Environmental*
1158 *Science and Pollution Research*, 29(32), 48908-48925.

1159 Katoch, M., Phull, S., Vaid, S., & Singh, S. (2017). Diversity, Phylogeny, anticancer and
1160 antimicrobial potential of fungal endophytes associated with *Monarda citriodora*
1161 L. *BMC microbiology*, 17, 1-13.

1162 Kaur, H.P., B. Singh, A., Kaur and S. Kaur, 2013. Anti-feedent and toxic activity of
1163 endophytic *Alternaria alternata* against tobacco caterpillar *Spodoptera litura*.
1164 *Journal of Pest Science*, 86: 543-550.

1165 Kaur, J., Sharma, A., Sharma, M. *et al.* (2019). Effect of α -glycosidase inhibitors from
1166 endophytic fungus *Alternaria destruens* on survival and development of insect
1167 pest *Spodoptera litura* Fab. and fungal phytopathogens. *Sci Rep* 9, 11400.
1168 <https://doi.org/10.1038/s41598-019-47838-6>

1169 Khalifa, A. G., Moselhy, W. A., Mohammed, H. M., Nabil, T. M., Shaban, M.,
1170 Aboelhadid, S. M., & Abdou, K. H. (2022). Toxicological evaluations of
1171 chitosan and silica nanoparticles loaded with deltamethrin with improved
1172 efficiency against *Culex pipiens* larvae. *International Journal of Environmental*
1173 *Science and Technology*, 1-20.

1174 Khalil, A. M. A., Hassan, S. E. D., Alsharif, S. M., Eid, A. M., Ewais, E. E. D., Azab,
1175 E., ... & Fouda, A. (2021). Isolation and characterization of fungal endophytes
1176 isolated from medicinal plant *Ephedra pachyclada* as plant growth-
1177 promoting. *Biomolecules*, 11(2), 140.

1178 Khursheed, A., Rather, M. A., Jain, V., Rasool, S., Nazir, R., Malik, N. A., & Majid, S.
1179 A. (2022). Plant based natural products as potential ecofriendly and safer
1180 biopesticides: A comprehensive overview of their advantages over conventional
1181 pesticides, limitations and regulatory aspects. *Microbial Pathogenesis*, 105854.

1182 Kowa, T. K., Jansen, O., Ledoux, A., Mamede, L., Wabo, H. K., Tchinda, A. T., ... &
1183 Frédérich, M. (2022). Bioassay-guided isolation of vilasinin-type limonoids and
1184 phenyl alkene from the leaves of *Trichilia gilgiana* and their antiplasmodial
1185 activities. *Natural Product Research*, 36(19), 5039-5047.

- 1186 Kumar, P., Shakya, R., Kumar, V., Kumar, D., Chauhan, R. P. S., & Singh, H. (2023).
1187 Chemical constituents and strong larvicidal activity of *Solanum xanthocarpum*
1188 among selected plants extracts against the malaria, filaria, and dengue
1189 vectors. *Journal of Vector Borne Diseases*, 60(1), 18-31.
- 1190 Kusumaningrum, H. P., Budi, W. S., Azam, M., & Bawono, A. (2014). Design of
1191 Electrophoresis Device for Optimization of DNA Visualization and DNA
1192 Concentration Using Software. *Jurnal Pendidikan Fisika Indonesia*, 10(2), 194-
1193 202.
- 1194 Lambrechts, L. (2023). Does arbovirus emergence in humans require adaptation to
1195 domestic mosquitoes?. *Current Opinion in Virology*, 60, 101315.
- 1196 Lanfranco, L., & Fiorilli, V. (2022). Life of Microbes Inside the Plant: Beneficial Fungal
1197 Endophytes and Mycorrhizal Fungi. *Good Microbes in Medicine, Food
1198 Production, Biotechnology, Bioremediation, and Agriculture*, 488-505.
- 1199 Lengai, G. M., Muthomi, J. W., & Mbega, E. R. (2020). Phytochemical activity and role
1200 of botanical pesticides in pest management for sustainable agricultural crop
1201 production. *Scientific African*, 7, e00239.
- 1202 Li, G., Kusari, S., Lamshoft, M., Schuffler, A., Laatsch, H., & Spiteller, M. (2014).
1203 Antibacterial secondary metabolites from an endophytic fungus, *Eupenicillium* sp.
1204 LG41. *Journal of natural products*, 77(11), 2335-2341.
- 1205 Li, Z., Ma, N., & Zhao, P. J. (2019). Acetylcholinesterase inhibitory active metabolites
1206 from the endophytic fungus *Colletotrichum* sp. YMF432. *Natural product
1207 research*, 33(12), 1794-1797.
- 1208 Lou, J., Fu, L., Peng, Y., & Zhou, L. (2013). Metabolites from *Alternaria* fungi and their
1209 bioactivities. *Molecules*, 18(5), 5891-5935.
- 1210 Magala P, Klevit RE, Thomas WE, Sokurenko EV, Stenkamp RE. RMSD analysis of
1211 structures of the bacterial protein FimH identifies five conformations of its lectin
1212 domain. *Proteins*. 2020 Apr;88(4):593-603. doi: 10.1002/prot.25840. Epub 2019
1213 Nov 5. PMID: 31622514; PMCID: PMC7058522.
- 1214 Mahmud, S. N., Sohrab, M. H., Begum, M. N., Rony, S. R., Sharmin, S., Moni, F., ... &
1215 Afroz, F. (2020). Cytotoxicity, antioxidant, antimicrobial studies and
1216 phytochemical screening of endophytic fungi isolated from *Justicia
1217 gendarussa*. *Annals of agricultural sciences*, 65(2), 225-232.

- 1218 Maliehe, T. S., Mbambo, M., Nqotheni, M. I., Senzo, N. S., & Shandu, J. S. E. (2022).
1219 Antibacterial effect and mode of action of secondary metabolites from fungal
1220 endophyte associated with *Aloe ferox* Mill. *Microbiology Research*, 13(1), 90-101.
- 1221 Mamboungou, J., Canedo, A., Qualhato, G., Rocha, T. L., & Vieira, L. G. (2022).
1222 Environmental risk of titanium dioxide nanoparticle and cadmium mixture:
1223 developmental toxicity assessment in zebrafish (*Danio rerio*). *Journal of*
1224 *Nanoparticle Research*, 24(9), 186.
- 1225 Manan, M.A., Rosfarizan, M., Ariff, A., 2017. The morphology and structure of red
1226 pigment producing fungus: *Monascus Purpureus*. *Microbiol. Exp* 5, 1-5. <https://doi.org/10.15406/jmen.2017.05.00138>.
- 1228 Manpreet Kaur, Neeraj Kumar Aggarwal & Romika Dhiman (2015) Screening of
1229 phytotoxicity of *Alternaria macrospora* MKP1 against *Parthenium*
1230 *hysterophorus* L., *Archives of Phytopathology and Plant Protection*, 48:17-20, 890-
1231 897, DOI: [10.1080/03235408.2016.1140567](https://doi.org/10.1080/03235408.2016.1140567)
- 1232 Masi, M., Cimmino, A., Tabanca, N., Becnel, J. J., Bloomquist, J. R., & Evidente, A.
1233 (2017). A survey of bacterial, fungal and plant metabolites against *Aedes aegypti*
1234 (Diptera: Culicidae), the vector of yellow and dengue fevers and Zika
1235 virus. *Open Chemistry*, 15(1), 156-166.
- 1236 Messina JP, Brady OJ, Golding N et al (2019) The current and future global distribution
1237 and population at risk of dengue. *Nat Microbiol* 4:508-1515.
1238 <https://doi.org/10.1038/s41564-019-0476-8>
- 1239 Mohamed, N. Z., Shaban, L., Safan, S., & El-Sayed, A. S. (2023). Physiological and
1240 metabolic traits of Taxol biosynthesis of endophytic fungi inhabiting plants: Plant-
1241 microbial crosstalk, and Epigenetic regulators. *Microbiological Research*, 127385.
- 1242 Narayanan, Z., & Glick, B. R. (2022). Secondary metabolites produced by plant growth-
1243 promoting bacterial endophytes. *Microorganisms*, 10(10), 2008.
- 1244 Narayanankutty, A., Sasidharan, A., Job, J. T., Rajagopal, R., Alfarhan, A., Kim, Y. O.,
1245 & Kim, H. J. (2021). Mango ginger (*Curcuma amada* Roxb.) rhizome essential
1246 oils as source of environmental friendly biocides: Comparison of the chemical
1247 composition, antibacterial, insecticidal and larvicidal properties of essential oils
1248 extracted by different methods. *Environmental Research*, 202, 111718.
- 1249 Natarajan D., Srinivasan R., and Shivakumar M. S. (2014). *Phyllanthus wightianus* Müll.
1250 Arg.: A Potential Source for Natural Antimicrobial Agents. *BioMed Research*

1251 International. Volume 2014, Article ID 135082, 9 pages
1252 <http://dx.doi.org/10.1155/2014/135082>.

1253 Nishimura Y, Murakami S, Ashikawa Y, Sasagawa S, Umemoto N, Shimada Y, Tanaka
1254 T (2015) Zebrafish as a system toxicology model for developmental
1255 neurotoxicity testing. *Congenit Anom* 55:1-16

1256 Nithya, K., Bhuvanaragavan, S., Sruthi, K., Meenakumari, M., Shanthi, S., & Janarthanan,
1257 S. (2022). Purification, characterization and larvicidal activity of a potent
1258 bioactive compound asarone from leaves of *Acorus calamus* against the culicid
1259 larval mosquitoes. *Parasitology International*, 90, 102620.

1260 OECD, 2013. Guideline for Testing of Chemicals, 236. Fish Embryo Acute Toxicity
1261 (FET) Test. OECD, Paris, France. Available at: Microsoft Word -
1262 1st Version FET Draft TG 30 May 2006.doc (oecd.org).

1263 Okagu, I. U., Okeke, E. S., Ezeorba, W. C. F., Ndefo, J. C., & Ezeorba, T. P. C.
1264 (2023). Overhauling the ecotoxicological impact of synthetic pesticides using plants'
1265 natural products: a focus on *Zanthoxylum* metabolites. *Environmental Science and*
1266 *Pollution Research*, 1-25.

1267 Parthiban, E., Bhuvanaragavan, S., Gonzalez-Ortega, O., Janarthanan, S., & Ramanibai, R.
1268 (2021). Mosquito larvicidal activity of *Ammona reticulata* extract and its lethal
1269 impacts on allelochemicals detoxifying enzymes in wild population dengue
1270 vector, *Aedes aegypti*. *International Journal of Pest Management*, 1-16.

1271 Pliego-Pliego E, Vasilieva O, Vela´zquez-Castro J et al (2020) Control strategies for a
1272 population dynamics model of *Aedes aegypti* with seasonal variability and their
1273 effects on dengue incidence. *Appl Math Model* 81:296-319.

1274 Podova, M., J. Dobias and P. Nemeč, 1977. Inhibitory effect of fungal metabolites on
1275 the development of *Drosophila melanogaster*. *Biologia (Bratislava)* 32: 657-662.

1276 Ragavendran, C., & Natarajan, D. (2015). Insecticidal potency of *Aspergillus terreus*
1277 against larvae and pupae of three mosquito species *Anopheles stephensi*, *Culex*
1278 *quinquefasciatus*, and *Aedes aegypti*. *Environmental Science and Pollution*
1279 *Research*, 22, 17224-17237.

1280 Ragavendran, C., Dubey, N. K., & Natarajan, D. (2017). *Beauveria bassiana*
1281 (Clavicipitaceae): a potent fungal agent for controlling mosquito vectors of
1282 *Anopheles stephensi*, *Culex quinquefasciatus* and *Aedes aegypti* (Diptera:
1283 Culicidae). *RSC advances*, 7(7), 3838-3851.

- 1284 Ragavendran, C., Manigandan, V., Kamaraj, C., Balasubramani, G., Prakash, J. S.,
1285 Perumal, P., & Natarajan, D. (2019). Larvicidal, histopathological, antibacterial
1286 activity of indigenous fungus *Penicillium* sp. against *Aedes aegypti* L and *Culex*
1287 *quinquefasciatus* (Say)(Diptera: Culicidae) and its acetylcholinesterase inhibition
1288 and toxicity assessment of zebrafish (*Danio rerio*). *Frontiers in Microbiology*, *10*,
1289 427.
- 1290 Rajagopalan, V., Venkataraman, S., Rajendran, D. S., Kumar, V. V., Kumar, V. V., &
1291 Rangasamy, G. (2023). Acetylcholinesterase biosensors for electrochemical
1292 detection of neurotoxic pesticides and acetylcholine neurotransmitter: A literature
1293 review. *Environmental Research*, 115724.
- 1294 Rants'o, T. A., Koekemoer, L. L., Panayides, J. L., & van Zyl, R. L. (2022). Potential of
1295 Essential Oil-Based Anticholinesterase Insecticides against Anopheles Vectors: A
1296 Review. *Molecules*, *27*(20), 7026.
- 1297 Sahiba, N., Sethiya, A., Soni, J., Teli, P., Garg, A., & Agarwal, S. (2022). A facile
1298 biodegradable chitosan-SO₃H catalyzed acridine-1, 8-dione synthesis with
1299 molecular docking, molecular dynamics simulation and density functional theory
1300 against human topoisomerase II beta and *Staphylococcus aureus* tyrosyl-tRNA
1301 synthetase. *Journal of Molecular Structure*, *1268*, 133676.
- 1302 Salamun, S., Susetyo, R. D., Nafidiastri, F. A., Zain, R. A., Sari, R. P., Geraldi, A., ... &
1303 Ni'matuzahroh, N. M. (2022). Potential biocontrol agent of indigenous *Bacillus*
1304 sp. EG6. 4: Molecular identification, larvicidal toxicity, and mechanism of
1305 actions. *Biodiversitas Journal of Biological Diversity*, *23*(10).
- 1306 Saleem, A., & El-Shahir, A. A. (2022). Morphological and molecular characterization
1307 of some *Alternaria* species isolated from tomato fruits concerning mycotoxin
1308 production and polyketide synthase genes. *Plants*, *11*(9), 1168.
- 1309 Sangeetha, K. D., & Ashtaputre, S. A. (2015). Morphological and cultural variability in
1310 isolates of *Alternaria* sp. causing leaf blight of cotton. *Karnataka J Agric*
1311 *Sci*, *28*(2), 214-219.
- 1312 Santra, H. K., & Banerjee, D. (2022). Broad-spectrum antimicrobial action of cell-free
1313 culture extracts and volatile organic compounds produced by endophytic fungi
1314 *Curvularia eragrostidis*. *Frontiers in Microbiology*, *13*, 920561.
- 1315 Santra, H. K., Maity, S., & Banerjee, D. (2022). Production of bioactive compounds
1316 with broad spectrum bactericidal action, bio-film inhibition and antilarval potential
1317 by the secondary metabolites of the endophytic fungus *Cochliobolus* sp. APS1

1318 isolated from the Indian medicinal herb *Andrographis*
1319 *paniculata*. *Molecules*, *27*(5), 1459.

1320 Schuller, A., Studt-Reinhold, L., & Strauss, J. (2022). How to completely squeeze a
1321 Fungus—Advanced genome mining tools for novel bioactive
1322 substances. *Pharmaceutics*, *14*(9), 1837.

1323 Selderslaghs IWT, Hooyberghs J, Blust R, Witters HE (2013) Assessment of the
1324 developmental neurotoxicity of compounds by measuring locomotor activity in
1325 zebrafish embryos and larvae. *Neurotoxicol Teratol* 37:44–56

1326 Sharma, D., Pramanik, A., & Agrawal, P. K. (2016). Evaluation of bioactive secondary
1327 metabolites from endophytic fungus *Pestalotiopsis neglecta* BAB-5510 isolated
1328 from leaves of *Cupressus torulosa* D. Don. *3 Biotech*, *6*(2), 210.

1329 Sharma, I., & Sharma, A. (2014). Use of *Alternaria* spp. as a pest control agent: A
1330 review. *World Appl Sci J*, *31*(11), 1869-72.

1331 Sharma, R., Shukla, A. C., & Tangiang, S. (2022). Fungal Endophytes: A Potential
1332 Source of Low-Cost Entrepreneurship. In *Applied Mycology* (pp. 39-73).
1333 Springer, Cham.

1334 Singab, A. N. B., Mostafa, N. M., Elkhawas, Y. A., Al-Sayed, E., Bishr, M. M., Elissawy,
1335 A. M., ... & Chang, F. R. (2022). Cyclodepsipeptides: Isolation from Endophytic
1336 Fungi of *Sarcophyton ehrenbergi* and Verification of Their Larvicidal Activity via
1337 In-Vitro and In-Silico Studies. *Marine Drugs*, *20*(5), 331.

1338 Singh, B., Thakur, A., Kaur, S., Chadha, B. S., & Kaur, A. (2012). Acetylcholinesterase
1339 inhibitory potential and insecticidal activity of an endophytic *Alternaria* sp. from
1340 *Ricinus communis*. *Applied biochemistry and biotechnology*, *168*, 991-1002.

1341 Sun, T., Wang, L., & Zhang, H. (2022). Intestinal microbiota in sepsis. *Intensive Care*
1342 *Research*, *2*(1-2), 1-7.

1343 Suneja, P., Kumar, P., Rani, S., & Dang, A. S. (2023). Identification of Fungal
1344 Endophytes by ITS rDNA Technique. In *Endophytic Microbes: Isolation,*
1345 *Identification, and Bioactive Potentials* (pp. 89-95). Humana, New York, NY.

1346 Taher, M. A., Tan, W. N., Chear, N. J. Y., Leong, C. R., Rashid, S. A., Tong, W. Y.,
1347 2022. Metabolites characterization of endophytic *Phyllosticta fallopiae* L67
1348 isolated from *Aloe vera* with antimicrobial activity on diabetic wound
1349 microorganisms. *Natural Product Res.* 1-6.

1350 Tajdini, M., Osouli, S., & Afsharmanesh, H. (2022). Evolution of the larvicidal effects of
1351 secondary metabolites produced by *Bacillus subtilis* (Ehrenberg, 1835) Cohn,

1352 1872 wild type UTB1 and mutant M419 against *Plutella xylostella* (L.,
1353 1758)(Lep.: Plutellidae). *Journal of the Entomological Research Society*, 24(3),
1354 257-268.

1355 Talukdar, R., Padhi, S., Rai, A. K., Masi, M., Evidente, A., Jha, D. K., ... & Tayung, K.
1356 (2021). Isolation and characterization of an endophytic fungus *Colletotrichum*
1357 *coccodes* producing tyrosol from *Houttuynia cordata* Thunb. using ITS2 RNA
1358 secondary structure and molecular docking study. *Frontiers in Bioengineering and*
1359 *Biotechnology*, 9, 650247.

1360 Tapwal, A., Pandey, P., & Chandra, S. (2015). Antimicrobial activity and phytochemical
1361 screening of endophytic fungi associated with *Cassia fistula*. *Int. J. Chem. Biol.*
1362 *Sci*, 2(7), 2349-2724.

1363 Thomma, B. P. (2003). *Alternaria* spp.: from general saprophyte to specific
1364 parasite. *Molecular plant pathology*, 4(4), 225-236.

1365 Toghueo, R. M. K. (2020). Bioprospecting endophytic fungi from *Fusarium* genus as
1366 sources of bioactive metabolites. *Mycology*, 11(1), 1-21.

1367 Tsuge, T., Harimoto, Y., Akimitsu, K., Ohtani, K., Kodama, M., Akagi, Y., ... & Otani,
1368 H. (2013). Host-selective toxins produced by the plant pathogenic fungus
1369 *Alternaria alternata*. *FEMS microbiology reviews*, 37(1), 44-66.

1370 Venkatesh, I., & Darvin, G. (2016). An overview on cotton *Alternaria* leaf spot and its
1371 management. *Int J Appl Bio Pharm Tech*, 7(2), 135.

1372 Vivekanandhan, P., Kavitha, T., Karthi, S., Senthil-Nathan, S., & Shivakumar, M. S.
1373 (2018). Toxicity of *Beauveria bassiana*-28 mycelial extracts on larvae of *Culex*
1374 *quinquefasciatus* mosquito (Diptera: Culicidae). *International journal of*
1375 *environmental research and public health*, 15(3), 440.

1376 Vivekanandhan, P., Swathy, K., & Shivakumar, M. S. (2022). Identification of
1377 insecticidal molecule aucubin from *Metarhizium anisopliae* ethyl acetate crude
1378 extract against disease mosquito vector. *International Journal of Tropical Insect*
1379 *Science*, 1-16.

1380 Vivekanandhan, P., Swathy, K., Kalaimurugan, D., Ramachandran, M., Yuvaraj, A.,
1381 Kumar, A. N., ... & Kweka, E. J. (2020). Larvicidal toxicity of *Metarhizium*
1382 *anisopliae* metabolites against three mosquito species and non-targeting
1383 organisms. *Plos one*, 15(5), e0232172.

1384 Vivekanandhan, P., Swathy, K., Murugan, A. C., & Krutmuang, P. (2022). Insecticidal
1385 efficacy of *Metarhizium anisopliae* derived chemical constituents against disease-
1386 vector mosquitoes. *Journal of Fungi*, 8(3), 300.

1387 Vu, T.H., Quach, N.T., Le, P.C. *et al.* (2023). Bioprospecting Endophytic Fungi
1388 Isolated from *Cephalotaxus mannii* Hook f. as Prolific Sources of Antibacterial,
1389 Anticancer, and Antioxidant Agents. *Microbiology* 92, 284–292.
1390 <https://doi.org/10.1134/S0026261722602834>

1391 WHO. (2023). *Report on insecticide resistance in Aedes mosquitoes (Aedes aegypti,*
1392 *Ae. albopictus, Ae. vittatus) in WHO South-East Asia Region countries* (No.
1393 SEA-CD-334). World Health Organization. Regional Office for South-East Asia.
1394 Licence: CC BY-NC-SA 3.0 IGO.

1395 Xing, Y. M., Chen, J., Cui, J. L., Chen, X. M., & Guo, S. X. (2011). Antimicrobial
1396 activity and biodiversity of endophytic fungi in *Dendrobium devonianum* and
1397 *Dendrobium thysiflorum* from Vietnam. *Current microbiology*, 62, 1218-1224.

1398 Yamany, A. S., Abdel-Ghaffar, F., Al Quraishy, S., Al-Amri, O., Mehlhorn, H., &
1399 Abdel-Gaber, R. (2022). Histological technique to detect the physiological age of
1400 the malaria vector mosquito *Anopheles pharoensis* (Diptera:
1401 Culicidae). *Microscopy Research and Technique*, 85(4), 1580-1587.

1402 Yang, F. Z., Li, L., & Yang, B. (2012). *Alternaria* toxin-induced resistance against rose
1403 aphids and olfactory response of aphids to toxin-induced volatiles of rose
1404 plants. *Journal of Zhejiang University Science B*, 13, 126-135.

1405 Zabouri, Y., Cheriguene, A., Chougrani, F., Merzouk, Y., Marchetta, A., Urzi, C., & De
1406 Leo, F. (2021). Antifungal activity of lactic acid bacteria against phytopathogenic
1407 *Alternaria alternata* species and their molecular characterization. *Journal of Food*
1408 *& Nutrition Research*, 60(1).

1409 Zhang, D., Sun, W., Xu, W., Ji, C., Zhou, Y., Sun, J., ... & Tian, Y. (2023).
1410 Antimicrobial and Cytotoxic Activity of Endophytic Fungi from *Lagopsis*
1411 *supina*. *Journal of Microbiology and Biotechnology*, 33(4), 543.

1412 Zibae, A., Bandani, A. R., & Tork, M. (2009). Effect of the entomopathogenic fungus,
1413 *Beauveria bassiana*, and its secondary metabolite on detoxifying enzyme activities
1414 and acetylcholinesterase (AChE) of the Sunn pest, *Eurygaster integriceps*
1415 (Heteroptera: Scutellaridae). *Biocontrol Science and Technology*, 19(5), 485-
1416 498.

1417

